

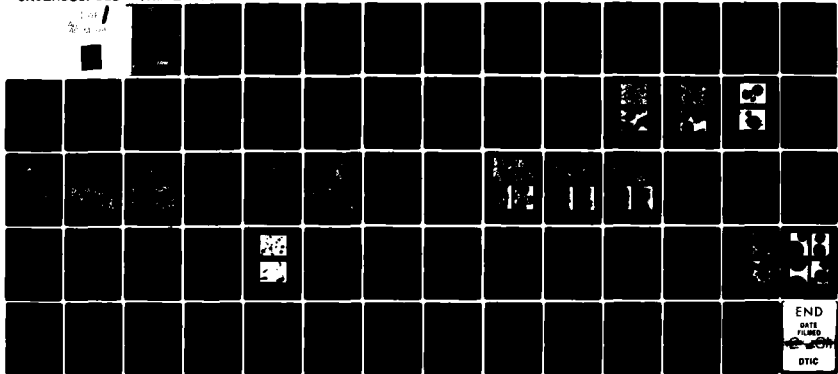
AD-A094 185

TRW INC CLEVELAND OH MATERIALS TECHNOLOGY
P/M PROCESSING OF RARE EARTH MODIFIED HIGH STRENGTH STEELS.(U)
DEC 80 A A SHEINKER

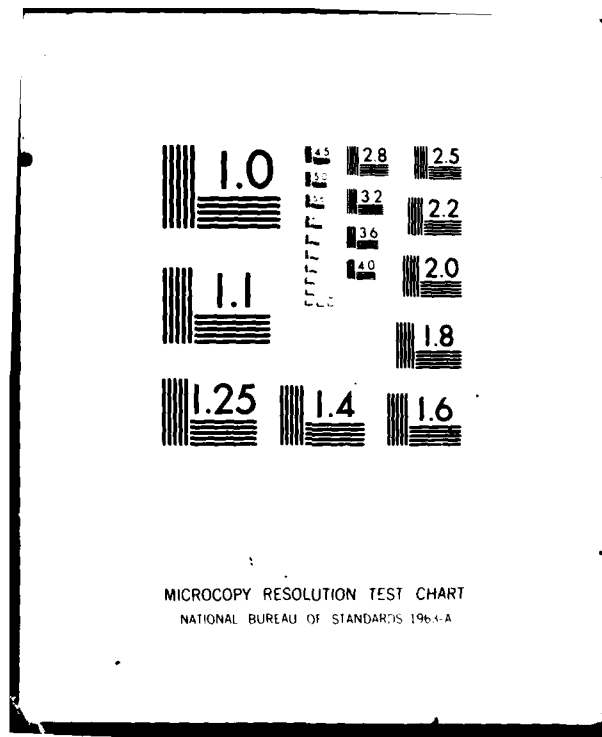
F/6 11/6
N00014-78-C-0672
NL

UNCLASSIFIED

TRW-ER-8097-2



END
DATE FILMED
DTIC



LEVEL

ER-8097-2

12

**P/M PROCESSING OF
RARE EARTH MODIFIED HIGH
STRENGTH STEELS**

By
A. A. SHEINKER

TECHNICAL REPORT

Prepared for
Office of Naval Research
Contract N00014-78-C-0672
NR 036-132

DTIC
JAN 27 1981

DECEMBER 1980

DISTRIBUTION STATEMENT A
Approved for public release;
Distribution Unlimited

TRW
EQUIPMENT
MATERIALS TECHNOLOGY

REPRODUCTION IN WHOLE OR IN PART IS PERMITTED
FOR ANY PURPOSE OF THE UNITED STATES GOVERNMENT

81136023

DOC FILE COPY

AD A 094185

UNCLASSIFIED

SECURITY CLASSIFICATION OF THIS PAGE (When Data Entered)

DD FORM 1 JAN 73 1473 EDITION OF 1 NOV 68 IS OBSOLETE
S N 0102-014-6601

UNCLASSIFIED 7/16/2023
SECURITY CLASSIFICATION OF THIS PAGE (When Data Entered)

UNCLASSIFIED

40-61

UNCLASSIFIED

UNCLASSIFIED (Classification of this page when Data Entered)

20. Abstract (continued)

at 2100°F (1420°K), but the ductility and impact resistance properties of the extruded powders were generally lower than those of similarly heat treated, rare earth modified, wrought 4340 steels evaluated previously, at approximately the same rare earth (cerium) content. Hot extrusion consolidation of 4340 steel powder which was mechanically alloyed with either 75% Ce-25% Ni or LaNi₅ alloy powders by attriting in a special high-intensity ball mill resulted in higher strength but lower ductility and impact resistance after heat treatment than the previously evaluated wrought 4340 steels at approximately the same rare earth content. Rapid solidification atomization of 4340 steel prealloyed with cerium by adding a 75% Ce-25% Ni alloy to the melt, using both the rapid solidification rate (RSR) and commercial rapid solidification (CRS) processes, resulted in very low cerium recoveries due to vaporization of the cerium in the RSR process and oxidation of the cerium in the CRS process. Because these difficulties could not be resolved within the scope of the program, no further work was performed on rapidly solidified powders.

4

Accession For	
NTIS GRA&I	
DTIC TAB	
Unannounced	
Justification	
By	
Distribution/	
Availability Codes	
Avail and/or	
Dist	Special

A

UNCLASSIFIED

ER-8097-2

TECHNICAL REPORT

**P/M PROCESSING OF
RARE EARTH MODIFIED HIGH STRENGTH STEELS**

Prepared for

Office of Naval Research
Contract N00014-78-C-0672
NR 036-132

December 1980

by

A. A. Sheinker

TRW Inc.
TRW Equipment
Materials Technology
Cleveland, Ohio 44117

FOREWORD

The work described in this report was performed in the Materials Technology Laboratory of TRW Inc., under the sponsorship of the Office of Naval Research, Contract N00014-78-C-0672. Dr. P. A. Clarkin acted as Program Monitor for the Navy. The program was administered for TRW by Dr. C. S. Kortovich, Program Manager. The Principal Investigator was Dr. A. A. Sheinker, with technical assistance provided by Mr. J. W. Sweeney and Mr. R. R. Ebert. The work conducted during the first year of this contract involved studies of material processing techniques for producing rare earth modified 4340 steel from metal powders. The work conducted during the second year, covered in this report, involved a continuation of these material processing studies.

This report has been assigned TRW Equipment Number ER-8097-2 and the data are recorded in laboratory notebook Number 794.

ABSTRACT

Material processing studies were continued directed toward developing powder metallurgy methods for producing rare earth modified high strength 4340 steel with improved resistance to hydrogen embrittlement. Three different methods of making rare earth modified 4340 steel powders were investigated: hydrogen gas atomization, mechanical alloying, and rapid solidification atomization. Hot extrusion consolidation of hydrogen gas atomized 4340 steel powders at 2150°F (1450°K) resulted in much better mechanical properties after heat treatment than hot isostatic pressing (HIP) consolidation at 2100°F (1420°K), but the ductility and impact resistance properties of the extruded powders were generally lower than those of similarly heat treated, rare earth modified, wrought 4340 steels evaluated previously, at approximately the same rare earth (cerium) content. Hot extrusion consolidation of 4340 steel powder which was mechanically alloyed with either 75% Ce-25% Ni or LaNi₅ alloy powders by attriting in a special high-intensity ball mill resulted in higher strength but lower ductility and impact resistance after heat treatment than the previously evaluated wrought 4340 steels at approximately the same rare earth content. Rapid solidification atomization of 4340 steel prealloyed with cerium by adding a 75% Ce-25% Ni alloy to the melt, using both the rapid solidification rate (RSR) and commercial rapid solidification (CRS) processes, resulted in very low cerium recoveries due to vaporization of the cerium in the RSR process and oxidation of the cerium in the CRS process. Because these difficulties could not be resolved within the scope of the program, no further work was performed on rapidly solidified powders.

TABLE OF CONTENTS

	<u>Page No.</u>
1.0 INTRODUCTION	1
2.0 PROGRAM OUTLINE	4
2.1 Powder Production and Characterization	4
2.1.1 Hydrogen Gas Atomization	4
2.1.2 Mechanical Alloying	6
2.1.3 Rapid Solidification Atomization	6
2.2 Powder Consolidation	7
2.3 Evaluation of Powder Processing	7
2.4 Selection of Optimum Powder Processing Conditions	7
3.0 PROGRAM STATUS	8
3.1 Hydrogen Gas Atomization	8
3.1.1 Experimental Procedures	8
3.1.2 Results and Discussion	13
3.1.3 Summary and Conclusions	31
3.2 Mechanical Alloying	33
3.2.1 Experimental Procedures	33
3.2.2 Results and Discussion	36
3.2.3 Summary and Conclusions	42
3.3 Rapid Solidification Atomization	42
3.3.1 Experimental Procedures	42
3.3.2 Results and Discussion	45
3.3.3 Summary and Conclusions	45
4.2 FUTURE WORK	50
4.1 Evaluation of Powder Processing	50
4.2 Selection of Optimum Powder Processing Conditions	50
4.3 Hydrogen Embrittlement Evaluation	50
4.3.1 Delayed Failure Testing	50
4.3.2 Hydrogen Content Analysis	51
4.3.3 Fractographic and Auger Analysis	52
5.0 REFERENCES	53

1.0 INTRODUCTION

The recent international conference on the effect of hydrogen on the behavior of metals at Jackson Lake Lodge, Wyoming, the third such conference in the past eight years, was an indication of the broad scope of the detrimental effects of hydrogen on engineering materials⁽¹⁾. Papers presented at this conference discussed the involvement of hydrogen in plasticity, fracture, fatigue, and environment assisted crack growth. Materials in which hydrogen damage was reported included a wide variety of steels, aluminum alloys, titanium alloys, nickel, cobalt and iron base superalloys, and a zirconium alloy. Among the engineering applications where hydrogen effects were cited as a problem were oil and gas wells, pipelines, pressure vessels, and electrical generators.

Hydrogen damage, specifically hydrogen embrittlement, in high strength steels is a particularly important problem because this class of materials is used in a wide range of critical applications where such damage could result in catastrophic failure. Thus, extensive efforts have been undertaken to develop methods of preventing hydrogen embrittlement in high strength steels. These approaches can be classified as microstructural alterations⁽²⁾, alloy composition modifications⁽²⁾, baking to remove hydrogen from the metal⁽³⁾, surface prestressing⁽⁴⁾, plating⁽⁵⁾, cathodic protection⁽⁶⁾, nonmetallic coating⁽⁷⁾, selective changes in surface composition by heat treatment⁽⁸⁾, and modification of the embrittling environment⁽⁹⁾. However, all of these methods involve serious limitations in practical applications, and no truly satisfactory method is currently available. A new approach which has considerable potential for controlling hydrogen embrittlement in high strength steels is the addition of rare earth elements to these materials.

Rare earth additions have been previously reported to control hydrogen damage in steels. The susceptibility to hydrogen blister or flake formation in 4340-type steels was reduced by adding 0.2 weight percent cerium, which formed stable hydrides below 1850°F (1280°K)⁽¹⁰⁾. The susceptibility to hydrogen-induced cracking of HY-80 steel weldments was decreased by combined additions of cerium and lanthanum (approximately 60 percent cerium and 40 percent lanthanum) at levels of 0.05, 0.09, and 0.13 weight percent^(11,12) with the maximum effect occurring at the 0.09 weight percent rare earth level^(11,12). More recently, delayed hydrogen cracking in HY-130 steel weldments was prevented in tests conducted to duplicate fabrication situations by the use of a Mischmetal (50 percent cerium, lanthanum, and small amounts of other rare earths) nickel cored wire as a second, cold-wire addition to the submerged-arc welding process⁽¹³⁾.

The feasibility of adding rare earths to high strength steels to improve hydrogen embrittlement resistance was demonstrated at TRW Materials Technology under ONR Contract No. N00014-74-C-0365⁽¹⁴⁾. In the first phase of this study, the hydrogen embrittlement cracking resistance of vacuum-induction melted 4340 steel containing about 0.05, 0.1 and 0.2 weight percent cerium or lanthanum was determined by sustained load delayed failure tests on cathodically charged and cadmium plated specimens. The results showed that at the 0.2 weight percent rare earth level, the threshold stress intensity (i.e., the stress intensity level below which failure did not occur) increased by a factor of about four and the crack growth rate decreased by about an order of magnitude as compared with 4340 steel without rare earth additions. This inhibition of hydrogen embrittlement cracking

was attributed to the interaction (possibly trapping) of the hydrogen with the rare earth elements, which reduced the amount of hydrogen available for embrittlement and crack growth at the tip of the crack.

In the second phase of this program, the concept of rare earth additions to high strength steels was extended to stress corrosion cracking behavior, because this type of failure in high strength steels is believed to be a form of hydrogen embrittlement⁽¹⁵⁾. Three heats of 4340 steel containing zero, 0.20, and 0.30 weight percent cerium were prepared and their resistance to stress corrosion cracking in 3.5 percent sodium chloride solution at room temperature was evaluated. The cerium additions had a much smaller effect on the stress corrosion cracking resistance than the cerium and lanthanum additions had on the hydrogen embrittlement cracking resistance in the previous study. The stress corrosion cracking threshold ($K_{I_{SCC}}$) was about the same for all three steels, but the higher cerium (0.30%) material had longer failure times and lower average crack growth rates than the lower cerium (0.20%) material. The failure times and average crack growth rates for the steel without cerium could not be directly compared with those for the two cerium-bearing steels because of crack branching which occurred only in the material without cerium. However, it was estimated that in the absence of branching, the failure times for the non-cerium steel would be shorter and the average crack growth rates higher than those of the lower cerium steel. The much smaller effect of the rare earth additions on the stress corrosion cracking resistance than on the hydrogen embrittlement cracking resistance was attributed to the proximity of the source of hydrogen to the crack tip during stress corrosion cracking. Since hydrogen enters the metal at the crack tip from the corrodent during stress corrosion cracking, the amount of hydrogen available for embrittlement is unlimited, and hydrogen transport into the crack tip is strongly influenced by metal-environment reactions at the crack tip surface rather than by diffusion through the metal.

A major limitation in these experimentally prepared rare earth modified high strength steels was a degradation in mechanical properties with increasing rare earth content. The decreases in strength were small, but the reductions in ductility and impact resistance were substantial, on the order of 30 percent for percent elongation, 40 percent for percent reduction of area, and 50 percent for Charpy impact energy at the 0.2 weight percent rare earth level. This degradation was attributed to the presence of nearly continuous networks of rare earth oxide inclusions at the prior austenite grain boundaries. These inclusions were apparently formed as a result of the combination of the highly reactive rare earth elements with the residual oxygen in the vacuum induction melting atmosphere and were not dispersed by extensive hot working of the steel ingots. The concentration of the rare earths in these large inclusions instead of a more uniform distribution was also suspected to have impaired their ability to interact with hydrogen and thus inhibit hydrogen embrittlement⁽¹⁶⁾. In order to overcome this problem, a method is required for incorporating the rare earth elements into the steel microstructure in a more homogeneous manner.

The objective of the current program being conducted under ONR Contract N00014-78-C-0672 is to develop a powder metallurgy method for making rare earth modified high strength steels with improved resistance to hydrogen embrittlement. The powder metallurgy approach offers a means of obtaining a more uniform distribution of the rare earth elements in the steel and minimizing the formation of rare earth oxide inclusions. This should improve the ductility and impact resistance and also enhance the hydrogen embrittlement resistance of rare earth modified high strength steels. During the first year of the program,

the research effort involved the development of material processing techniques for producing rare earth modified 4340 steel from metal powders^[17]. Three different methods of making rare earth modified 4340 steel powders were explored: hydrogen gas atomization, mechanical alloying, and rapid solidification rate atomization. These studies included metallographic characterization of powders made by all three of these methods and preliminary mechanical property evaluation of compacted material made from hydrogen gas atomized powder. Hydrogen gas atomization of 4340 steel prealloyed with cerium by adding a 75%Ce - 25%Ni alloy to the melt produced powder particles which were irregular in shape, clean, and relatively free of nonmetallic inclusions. The mechanical properties of this powder material consolidated by hot isostatic pressing (HIP) at 2000°F (1370°K) were generally lower than those of similarly heat treated, rare earth modified, wrought 4340 steels evaluated previously, due to a brittle condition in the prior particle boundaries of the compacted material. Mechanical alloying of hydrogen gas atomized 4340 steel powder containing no rare earths with either 75%Ce - 25%Ni or LaNi₅ alloy powders by attriting in a special high-intensity ball mill showed that annealing of the steel powder prior to attriting was necessary in order for the attriting to be effective. Rapid solidification rate (RSR) atomization of a control heat of 4340 steel with no rare earth additions produced powder particles which were generally spherical in shape, clean, and relatively free of nonmetallic inclusions, but contained many internal voids. The solidification patterns on the RSR particle surfaces were generally dendritic, as compared with those on the surfaces of the hydrogen gas atomized powder particles which were equiaxed, but no differences in the microstructures of these two types of powders could be discerned by light microscopy. This report describes the work conducted during the second year of the program. This work involved the continuation of the material processing studies described above.

2.0 PROGRAM OUTLINE

The objective of this program is the development of powder metallurgy methods for the production of rare earth modified high strength steels with improved resistance to hydrogen embrittlement. To accomplish this, work is being directed towards evaluating the applicability of various powder metallurgy processing techniques including appropriate consolidation methods for the production of rare earth modified 4340 steel powders. Current efforts involve a detailed study of these processing approaches, and a flow chart outlining this portion of the program is presented in Figure 1. Three different techniques for making the metal powders are being explored: hydrogen gas atomization, mechanical alloying, and rapid solidification atomization. These three methods were chosen because of their potential for producing a uniform distribution of the rare earth elements in the steel and minimizing the formation of rare earth oxide inclusions. The rare earth elements cerium and lanthanum were selected for this study on the basis of the previous work conducted at TRW which showed improved resistance to hydrogen embrittlement when either of these elements was added to 4340 steel⁽¹⁴⁾.

2.1 Powder Production and Characterization

2.1.1 Hydrogen Gas Atomization

The first approach involves hydrogen gas atomization of 4340 steel prealloyed with cerium by adding a 75% cerium - 25% nickel alloy to the melt. The hydrogen gas atomization process is a proven method of producing special alloy powders with low oxygen contents⁽¹⁸⁾. The most commonly used method of making low alloy steel powders, water atomization, is not acceptable because the oxygen content of the powder produced by this process is in excess of 1000 ppm⁽¹⁹⁾. This high oxygen level is expected to result in the formation of massive rare earth oxide inclusions during subsequent powder processing. This first approach involves the preparation of a number of heats of hydrogen gas atomized 4340 steel powder to obtain a concentration of 0.2 percent cerium in the powder. This cerium level was chosen because maximum improvement in hydrogen embrittlement resistance occurred at this level in the previous study⁽¹⁴⁾. An additional heat of hydrogen gas atomized 4340 steel powder is made with no rare earth addition for control purposes.

The hydrogen gas atomized 4340 steel powders are characterized by means of analysis of the chemical composition and metallographic examination of the microstructure. The main purpose of the chemical analyses is to determine the rare earth content of these powders and thus evaluate the degree of recovery of rare earth additions. The metallographic analyses include light microscopy, scanning electron microscopy, and electron microprobe analysis. The scanning electron microscopy is used to examine the characteristics of the loose powder particles, including their shape and overall size distribution. The light microscopy and electron microprobe analysis are used to examine the microstructure of the powder particles and to determine the location of the rare earth phases in the microstructure, as well as the degree of chemical segregation and the presence of impurities.

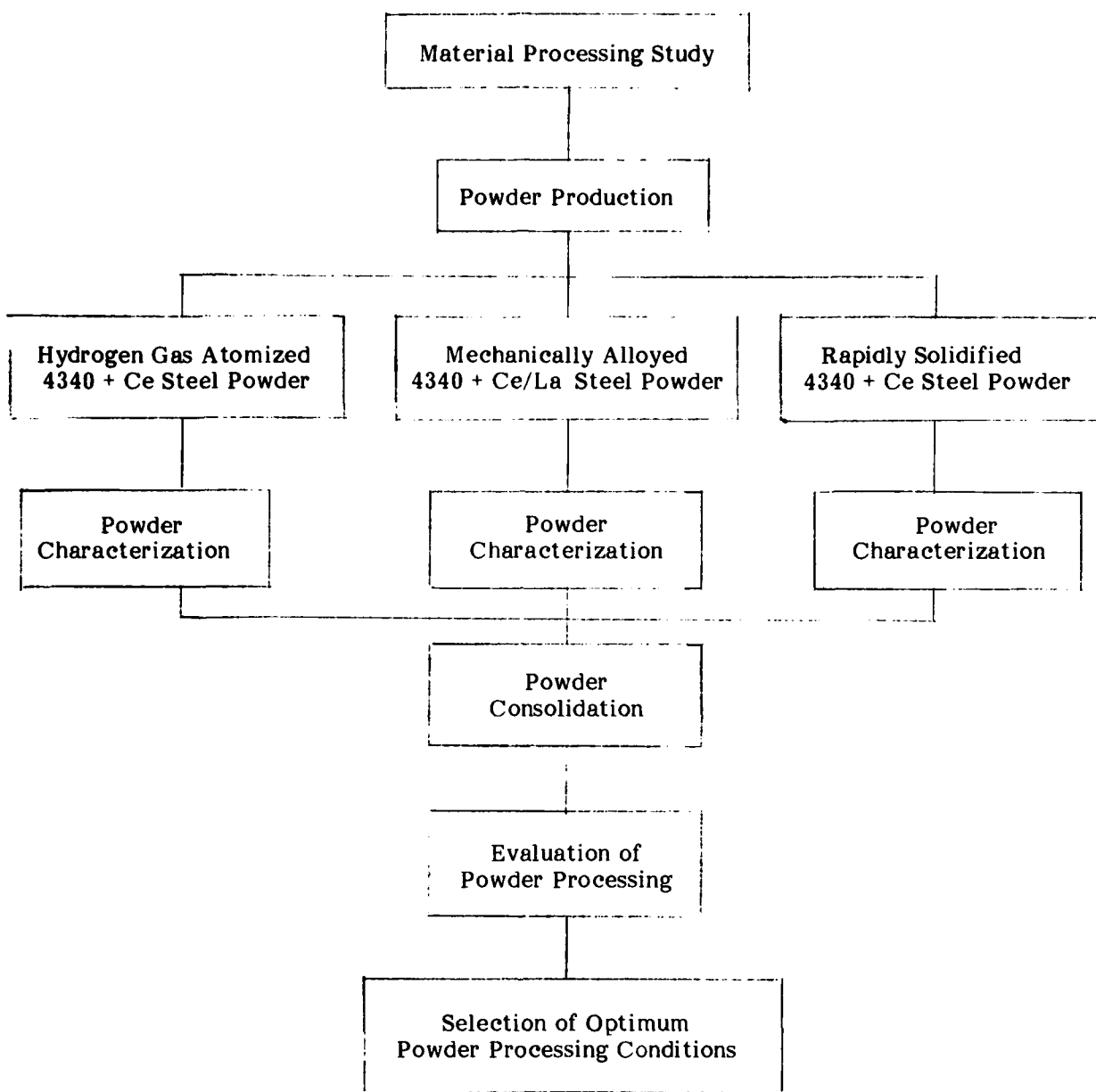


Figure 1. Flow Diagram of Current Program.

2.1.2 Mechanical Alloying

The second approach involves mechanical alloying of hydrogen gas atomized 4340 steel powder with either 75% cerium -25% nickel alloy powder or lanthanum-nickel (LaNi₅) powder at a level of 0.2 weight percent. Mechanical alloying is a relatively new technique⁽²⁰⁻²²⁾ for forming alloys which cannot be produced by conventional melting methods. Mechanical alloying is accomplished by attriting different metal powders in a special high-intensity ball mill resulting in a uniform distribution of alloying elements throughout the microstructure. In this second approach, six preliminary attriting trials are conducted in which the amount of rare earth compound powder added, the attriting ball size, the ball/powder ratio, and the attriting time are varied to produce optimum mechanical alloying, i.e., a uniform distribution of the rare earth additions in the steel microstructure. Lanthanum was chosen as an additional rare earth element for the mechanical alloying study because of the availability of the LaNi₅ alloy which was specially developed for hydrogen absorption capability by the International Nickel Company⁽²³⁾. Lanthanum was also effective in improving the hydrogen embrittlement resistance of 4340 steel in the previous study⁽¹⁴⁾. Using the optimum mechanical alloying conditions established in the preliminary attriting runs, three final attriting runs are made with sufficient powder for subsequent consolidation and mechanical property evaluation. In these three runs, the 4340 steel powder is attrited with (1) cerium-nickel powder, (2) LaNi₅ powder, and (3) no earth addition for control purposes.

The attrited powders from both the preliminary and final runs are characterized by chemical and metallographic analyses. The chemical analyses are used mainly to measure the rare earth content of these powders and hence determine the degree of recovery of the rare earth additions. The metallography involves light microscopy, scanning electron microscopy, and electron microprobe analysis. The scanning electron microscopy is utilized in examining the characteristics of the attrited powder particles, including their shape and overall size distribution. The light microscopy and electron microprobe analysis are used in examining the microstructure of the powder particles and in determining the degree of mechanical alloying as characterized by the deformation and fracture of the particles.

2.1.3 Rapid Solidification Atomization

The third method investigated was rapid solidification rate (RSR) atomization of 4340 steel prealloyed with cerium by adding a 75% cerium - 25% nickel alloy to the RSR melt. The RSR process is a newly developed technique for making high quality metal powders which enables more effective alloying and minimizes chemical segregation in the powder⁽²⁴⁻²⁶⁾. This process allows the addition of greater quantities of alloying elements without the accompanying segregation effects which have proven detrimental to both subsequent processing and mechanical properties. Thus it is believed that the rapidly solidified steel powders can be alloyed with relatively large amounts of rare earth additions without the formation of massive grain boundary inclusions. This third approach involves the preparation of two heats of RSR atomized 4340 steel powder, one containing 0.2 percent cerium and the other with no rare earth addition for control purposes.

The RSR approach to making rare earth modified 4340 steel powders was discontinued during the course of second year of the program because of a very low (0.0019%) cerium recovery in the cerium-bearing RSR powders. This low recovery was attributed to vaporization of the cerium during melting of the charge and subsequent superheating of the melt, since it was necessary to add the cerium-nickel prior to heating the charge. This problem could not be resolved within the scope of the current program because no provision was available for adding alloying elements to the melt just before atomization on any of the existing RSR atomization facilities.

2.2 Powder Consolidation

Following powder characterization, the powders are consolidated by either hot isostatic pressing (HIP)⁽²⁷⁾ or hot extrusion. The processes were selected for powder consolidation because of their potential for producing a favorable compacted microstructure, including a fully dense structure, no incipient melting, and a uniform distribution of rare earths. The most commonly used method of compacting low alloy steel powders, pressing and sintering, is not employed because steel powders produced by hydrogen gas atomization or RSR atomization are difficult to sinter⁽²⁸⁾. A number of consolidation operations are performed in which temperature is varied to determine the optimum temperature for obtaining the most favorable microstructure. The consolidated powders are evaluated metallographically to determine whether favorable compacted microstructures have been obtained.

2.3 Evaluation of Powder Processing

The consolidated powders are heat treated and then evaluated by light metallography and mechanical property tests which include tensile and Charpy impact tests conducted at room temperature. Duplicate tensile and Charpy impact tests are performed on compacts of five different types of 4340 steel powder: (1) hydrogen gas atomized powder with and without cerium; and (2) attrited powder with cerium, lanthanum, and no rare earths. The specific processing conditions chosen for this testing depend on the results of the metallographic analyses of the powder compacts. The test specimens are heat treated to a yield strength level of approximately 200 ksi (1400 MPa) by austenitizing, quenching, and tempering at 450°F (505°K) for comparison with the previous results on rare earth modified 4340 steel⁽¹⁴⁾.

2.4 Selection of Optimum Powder Processing Conditions

The final step in this material processing study is the selection of the optimum powder processing conditions. This selection is made on the basis of the metallographic and mechanical property evaluations of the powder metal compacts. These processing conditions include attriting parameters and consolidation temperature.

3.0 PROGRAM STATUS

During the first and second years of the program, the research effort involved the development of material processing techniques for producing rare earth modified 4340 steel from metal powders. Work was conducted on all three approaches for making the metal powders, hydrogen gas atomization, mechanical alloying, and rapid solidification rate atomization, and the efforts in the first two of these three areas are continuing. The details of this work are described in the following sections.

3.1 Hydrogen Gas Atomization

3.1.1 Experimental Procedures

3.1.1.1 Powder Preparation

The hydrogen gas atomization process for making metal powders involves supersaturating the melt with highly pressurized hydrogen and imploding the gas-saturated molten metal through an orifice into a vacuum chamber, where the stream of pressurized liquid metal erupts into particles⁽¹⁸⁾. The resulting powder particles are generally irregular in shape rather than spherical. The advantages of this method of atomization are thorough mixing occurring during melting, low porosity levels in the powder particles, and low oxygen contents (generally less than 100 ppm) in the powder product.

As reported in the previous report on this program⁽¹⁷⁾, four heats of 4340 steel powder were made by the hydrogen gas atomization process at Homogeneous Metals, Inc., under subcontract to TRW. The melt stock for these heats was vacuum-induction melted and aluminum deoxidized 4340 steel without rare earths. The cerium was added to the melt in the form of irregularly-shaped, roughly 0.05-inch (0.001-m) diameter granules of a 75% cerium - 25% nickel alloy just before atomization⁽¹⁷⁾. The complete chemical compositions of these heats were given in the previous report⁽¹⁷⁾. The cerium contents of these four heats are presented in Table 1. One of these heats (X916) was a control heat containing no rare earth elements, while one other heat was to contain approximately 0.2% cerium. The first cerium heat attempted (X917) contained much less cerium than the desired level because the degree of cerium recovery in these powders was much lower than had been anticipated. This necessitated a second atomization iteration (X971) which was also disappointing. A third heat was required to obtain powder with 0.2% cerium content. However, the extra two heats were useful in the powder consolidation studies. All four heats of powder were screened to -80 mesh size for subsequent processing.

3.1.1.2 Powder Consolidation

During the first year of the program, powders from heats X916 and X917 were consolidated by the HIP process at Industrial Materials Technology, Inc., under subcontract to TRW. The HIP process consisted of enclosing the powder in a can and outgassing, sealing the can under vacuum, and holding the can in an autoclave at a high temperature and a high pressure for a specified length of time⁽²⁷⁾. After removing the can from the autoclave, the can material was removed from the compacted powder by machining or chemical dissolution. In this program, round cylindrical carbon steel HIP cans were

Table 1

Cerium Contents of Hydrogen Gas Atomized 4340 Steel Powders
Weight Percent

<u>Heat Number</u>	<u>Cerium Content, %</u>
X916	0
X917	0.004
X971	0.043
X989	0.24

employed to produce round bar powder compacts. For the powders from heats X916 and X917, the HIP consolidation was conducted at a pressure of 15,000 psi (103 MPa) for 2 hours and at temperatures of 1800 and 2000°F (1260 and 1370°K). The HIP'ed bars measured 9/16 inch (0.014 m) in diameter by 9 inches (0.23 m) long after the can material was removed by machining on a lathe.

During the second year of the program, an additional HIP operation was performed at 2100°F (1420°K) and at the same pressure for the same length of time as the previous HIP operations. This HIP run was conducted at 2100°F (1420°K) because the 1800°F (1260°K) HIP temperature had resulted in incomplete compaction of the powder and the 2000°F (1370°K) HIP temperature had resulted in poor mechanical properties⁽¹⁷⁾. This additional HIP operation was performed on powder from heat X989 to produce two round bars of the same dimensions as the bars from the previous HIP runs. Also, all six of the bars which had been HIP'ed previously at 1800°F (1260°K), including three bars of heat X916 powder and three bars of heat X971 powder, were re-HIP'ed at 2100°F (1420°K) in this operation, in order to more completely consolidate these bars and obtain satisfactory HIP'ed material with the lower cerium contents.

The 2100°F (1420°K) HIP operation gave disappointing mechanical properties and hot extrusion was added in the program for powder consolidation. Powders from heats X917 and X989 were consolidated by hot extrusion using the extrusion can configuration illustrated in Figure 2. The cans were made of type 304 stainless steel. First, the bottom was welded to the body of the can using the gas tungsten arc (GTA) process. The open can, the lid, a 2-1/2-inch (0.0635-m) diameter by 1/8-inch (0.0032-m) thick type 304 stainless steel disk, and the steel powders were then placed in a GTA welding chamber. The chamber was evacuated overnight and then back-filled with argon. Next, the can was filled with 4 pounds (1.8 kg.) of the powder and the disk was placed over the powder to act as a baffle to prevent the escape of powder during subsequent evacuation of the can. The lid was then GTA welded to the top of the extrusion can. Next, the sealed can was transferred to an electron beam welding chamber which was then evacuated. A small hole was drilled through the center of the lid of the can using a focused electron beam. In order to minimize the presence of adsorbed argon, the powder was vacuum outgassed by heating to 1000°F (810°K) and evacuating the heated can to 10^{-4} torr for 8 hours. Heating was accomplished by means of an induction coil surrounding the can, as shown in Figure 3. The can was then allowed to cool to room temperature and the small hole in the lid of the can was closed using a defocused electron beam. The sealed can was then removed from the electron beam welding chamber. The can was heated in a furnace to the desired extrusion temperature and held at the temperature for one hour. Finally, the powder-filled can was transferred within 10 seconds to a 700-ton (6-MN) Loewy hydraulic extrusion press where the powder was extruded through a conical die.

The hydrogen gas atomized powders from heats X917 and X989 were extruded at a temperature of 2150°F (1450°K) and an extrusion ratio of 16:1. This extrusion temperature was selected because satisfactory steel powder extrusions are usually obtained by extruding the powder at the normal forging temperature of the steel, and 2150°F (1450°K) is the typical forging temperature for wrought 4340 steel. This operation produced round bar stock measuring 3/4-inch (0.019-m) in diameter by approximately 36-inches (0.91-m) long. The net diameter of the extruded 4340 steel bar was 5/8-inch (0.016-m) after the can material was removed by machining on a lathe. One extrusion was made from each of

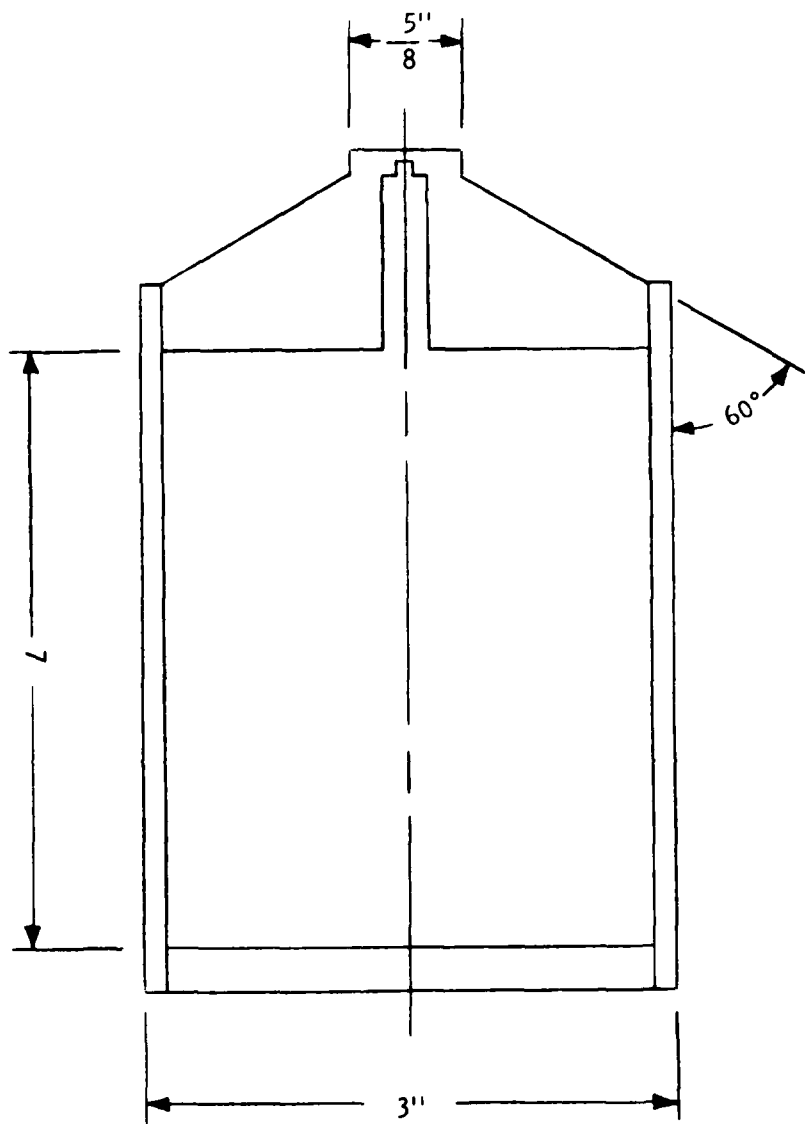


Figure 2. Metal powder extrusion can.

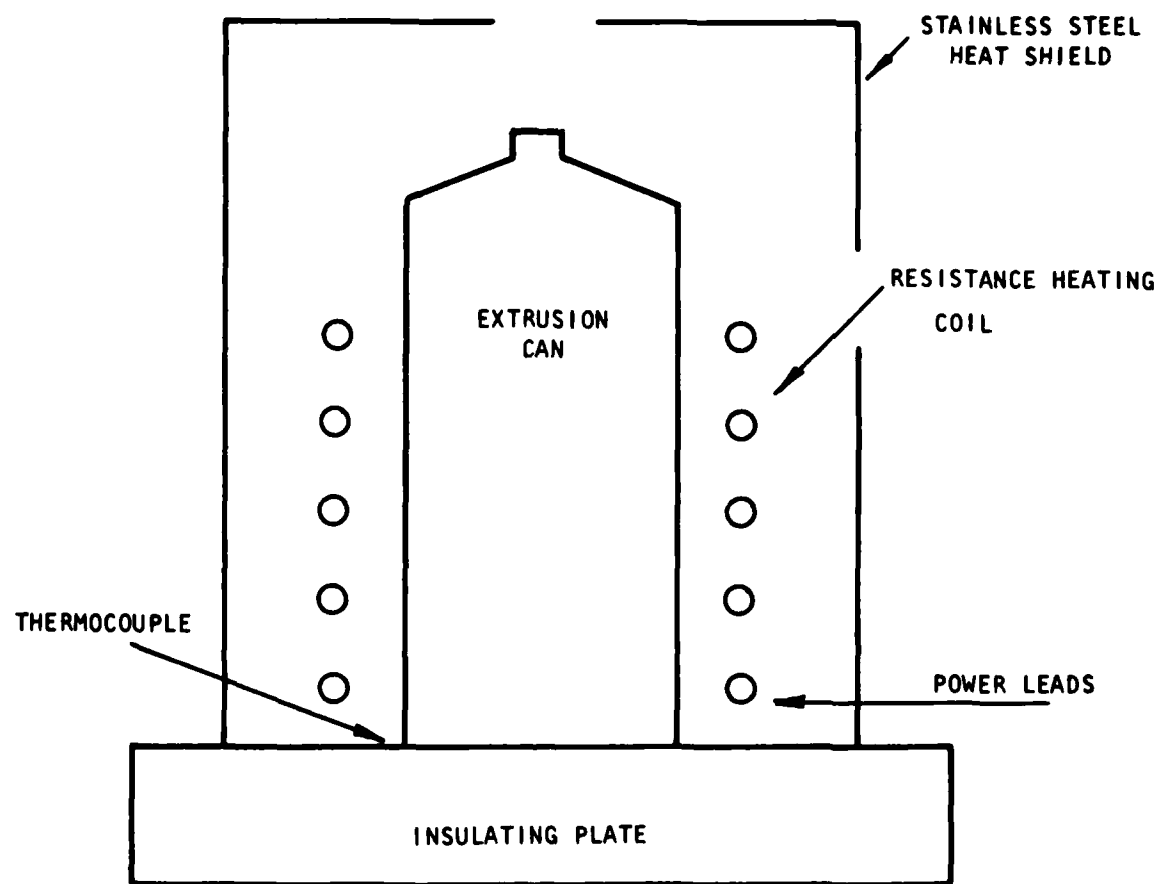


Figure 3. Schematic illustration of apparatus inside electron beam welding chamber for vacuum outgassing of extrusion billets.

the two heats of hydrogen gas atomized powder. No powder from heat X971 was extruded because this powder contained much less cerium (0.043%) than the desired level.

3.1.1.3 Powder Evaluation

Both the HIP'ed and extruded powder compacts were evaluated by metallographic analysis and mechanical property tests on heat treated specimens. The metallographic analyses were performed on 1/4-inch (0.0064-m) thick slices cut from the bars. The mechanical properties of the bars were evaluated by performing duplicate tensile and Charpy impact tests at room temperature on specimens machined from these bars. In two cases where the scatter in the tensile test results was large, an additional tensile specimen was tested. The mechanical property test matrix is presented in Table 2. The dimensions of the tensile and Charpy impact specimens are shown in Figure 4. These test specimens were rough machined from the bars, heat treated, and then finish ground to their final dimensions. The heat treatment consisted of the following:

1. Normalize at 1700°F (1200°K) for 15 minutes in argon atmosphere and air cool.
2. Austenitize at 1550°F (1120°K) for 30 minutes in argon atmosphere and oil quench.
3. Temper at 450°F (505°K) for 1 hour plus 1 hour in air, and air cool.

The 450°F (505°K) tempering temperature was chosen for comparison with the previous results on rare earth modified 4340 steel⁽¹⁴⁾.

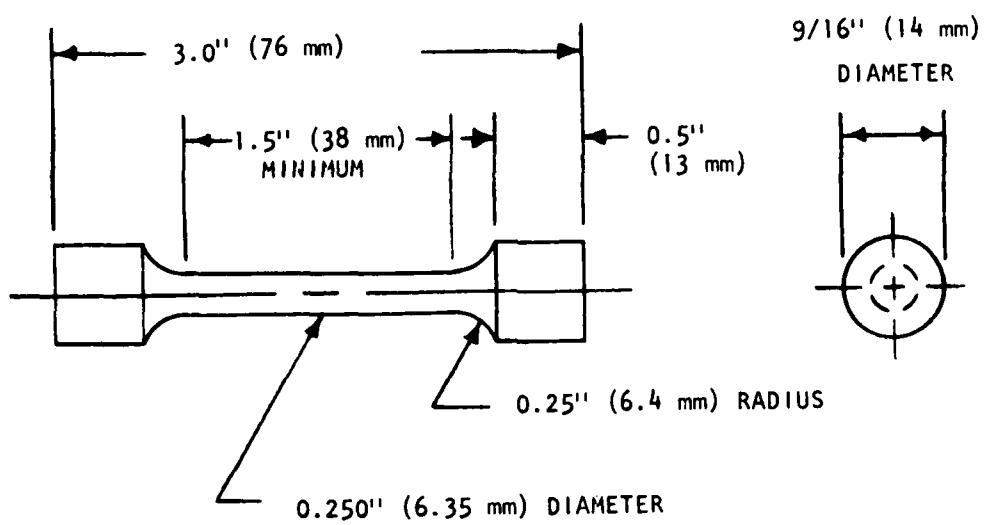
3.1.2 Results and Discussion

3.1.2.1 Powder Characterization

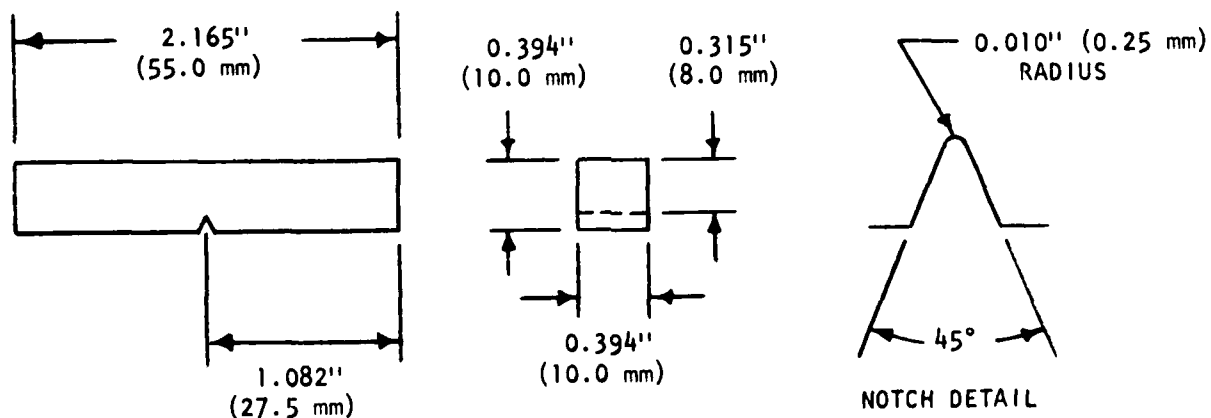
The characterization of the powders from heats X916 and X917 was described previously⁽¹⁷⁾. For heats X971 and X989, photographs taken in the scanning electron microscope of samples of the loose powders are shown in Figures 5 and 6, respectively. The irregularly shaped powder particles and smaller satellite particles attached to larger particles are typical of powders made by the hydrogen gas atomization process^(18,29). However, a larger proportion of the particles in heats X971 and X989 appeared to be spherically shaped than in heats X916 and X917. This was probably due to the addition of argon to the atomizing gas (50% H₂ + 50% Ar) for heats X971 and X989. Argon was added to the atomizing gas for these two heats to increase the yield of -80 mesh powder because this yield for the first two heats (X916 and X917) was low (about 30% of input)⁽¹⁷⁾. No significant differences in the size or shape of the particles were observed between the powders from heats X971 and X989. These powders appeared to be clean and relatively free of nonmetallic inclusions, as indicated by the light photomicrographs shown in Figure 7. No differences were observed in the light microscope between these two heats of powder.

Table 2
Mechanical Property Test Matrix

<u>Heat Number</u>	<u>Bar Number</u>	<u>Cerium Content %</u>	<u>Number of Tensile Specimens</u>	<u>Number of Charpy Impact Specimens</u>
<u>Bars HIP'ed at 1800^oF (1260^oK) and Re-HIP'ed at 2100^oF (1420^oK)</u>				
X916	9G253A	0	1	1
X916	9G253B	0	2	1
X971	9G254A	0.043	1	1
X971	9G254B	0.043	1	1
<u>Bars HIP'ed at 2100^oF (1420^oK)</u>				
X989	80B157	0.24	1	1
X989	80B158	0.24	2	1
<u>Bars Extruded at 2150^oF (1450^oK)</u>				
X917	5	0.004	2	2
X989	6	0.24	2	2

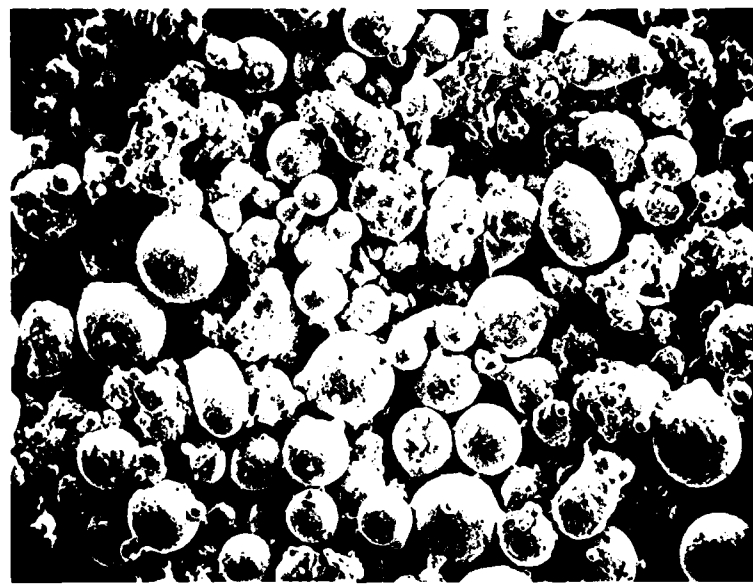


(a) Tensile test specimen.

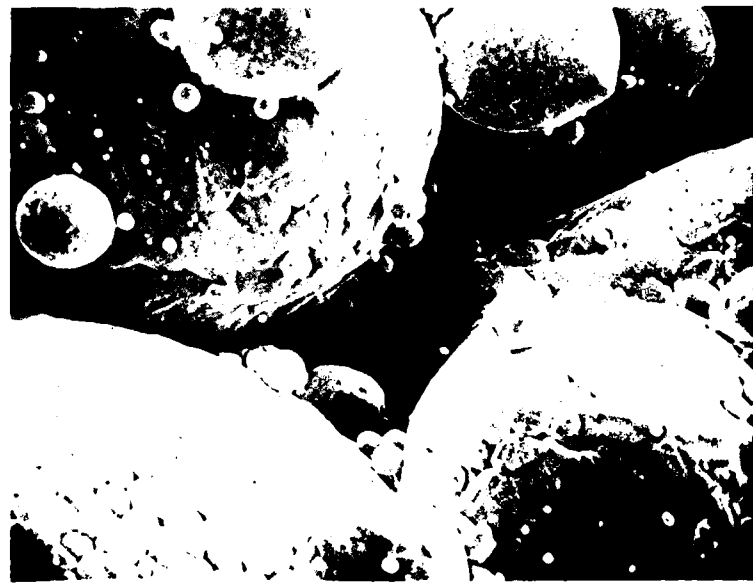


(b) Charpy impact test specimen.

Figure 4. Tensile and Charpy impact test specimens used to evaluate mechanical properties of powder metallurgy 4340 steels.

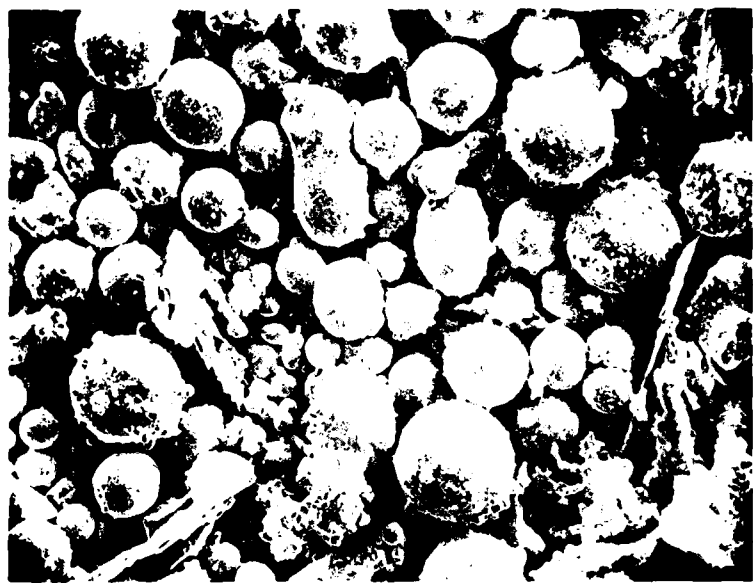


(a) Magnification, 100X



(b) Magnification, 1000X

Figure 5. SEM photographs of hydrogen gas atomized 4340 steel powders of Heat X971 (0.043% Ce).

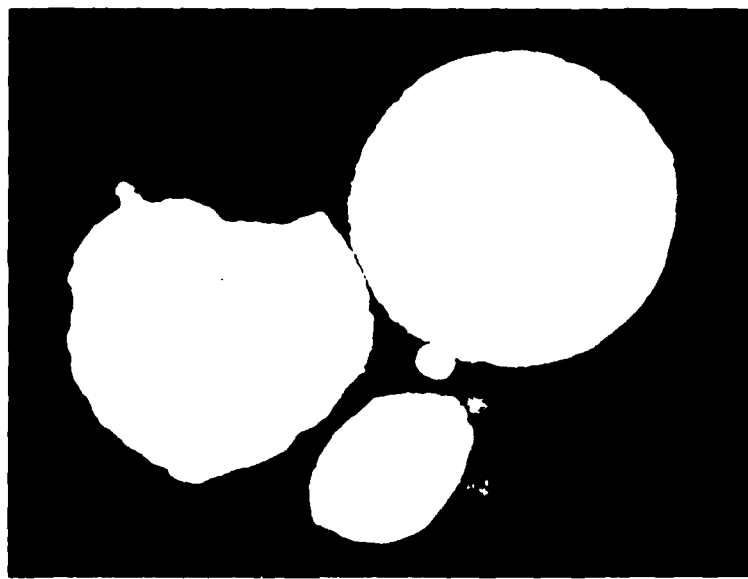


(a) Magnification, 100X

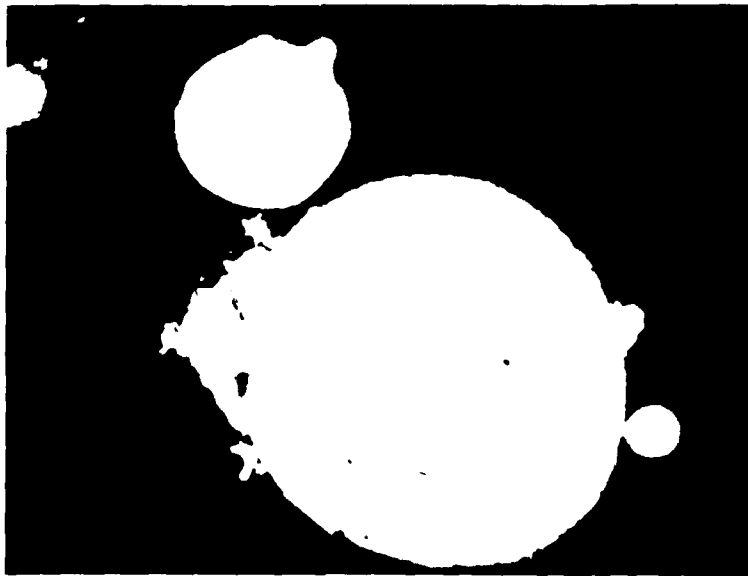


(b) Magnification, 1000X

Figure 6. SEM photographs of hydrogen gas atomized 4340 steel powders of Heat X989 (0.24% Ce).



(a) Heat X971 (0.043% Ce)



(b) Heat X989 (0.24% Ce)

Figure 7. Light photomicrographs of unetched hydrogen gas atomized 4340 steel powders, Magnification, 500X.

Electron microprobe analysis of the powder from heat X989, which contained 0.24 percent cerium, revealed that cerium was present in approximately 20 percent of the powder particles and was located more often at the surface of the particles than in the interior. The cerium in these particles was always concentrated in a very small area, suggesting the presence of a very small cerium-bearing phase, and was usually associated with a higher oxygen content than that in the remainder of the powder particle. As reported previously⁽¹⁷⁾, the oxygen contents of the four heats of hydrogen gas atomized powder were all higher than had been anticipated (>100 ppm) and increased with increasing cerium content, ranging from 142 ppm for the heat without cerium (X916) to 900 ppm for the heat with 0.24% cerium (X989). This was attributed to the strong oxygen getter behavior of cerium, which apparently combined with the residual oxygen in the controlled atmospheres during melting and atomization.

3.1.2.2 Powder Consolidation

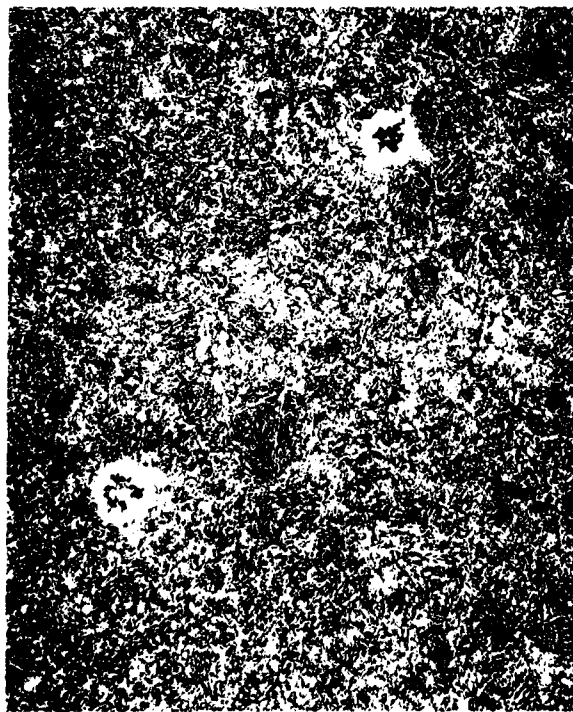
3.1.2.2.1 HIP Consolidation

Photomicrographs of the bars which were HIP'ed or re-HIP'ed at 2100°F (1420°K) are shown in Figures 8, 9, and 10 in the as-HIP'ed condition. These bars were consolidated from powder from (1) heat X989 containing 0.24% cerium, Figure 8, (2) heat X916 containing no cerium and HIP'ed previously at 1800°F (1260°K), Figure 9, and (3) heat X971 containing 0.043% cerium and HIP'ed previously at 1800°F (1260°K), Figure 10. There was some evidence of incomplete compaction in all three of these bars, as indicated by the unetched photomicrographs in Figures 8a, 9a, and 10a, but this condition did not appear to be as extensive as in the material HIP'ed at 1800°F (1260°K) only⁽¹⁷⁾. This condition would be expected to be detrimental to mechanical properties because of the effect of the large voids between incompletely bonded particles. Another type of defect, cross contamination particles, was observed in these three bars, as shown by the etched photomicrographs in Figures 8, 9, and 10. These particles did not respond to the etching as the steel did, suggesting that they may have been from a different alloy. Electron microprobe analysis of similar particles in material HIP'ed at 2000°F (1370°K) (heat X971, bar 9G254D) revealed that they contained W, Ti, Cb, and Co, elements which are not in the standard 4340 steel composition, as well as higher concentrations of Ni, Cr, Mo, Mn, and Si than in the 4340 steel matrix. This confirmed that these particles were cross contaminants. The presence of these foreign particles in the material indicated that the powder production equipment was not entirely free of particles remaining from previous operations with other alloys. Contaminant particles such as these can be detrimental to mechanical properties, particularly those properties which involve a crack initiation and growth process, such as fatigue strength and hydrogen embrittlement resistance⁽³⁰⁾. However, these particles did not appear to affect the tensile or Charpy impact properties of the HIP'ed bars.

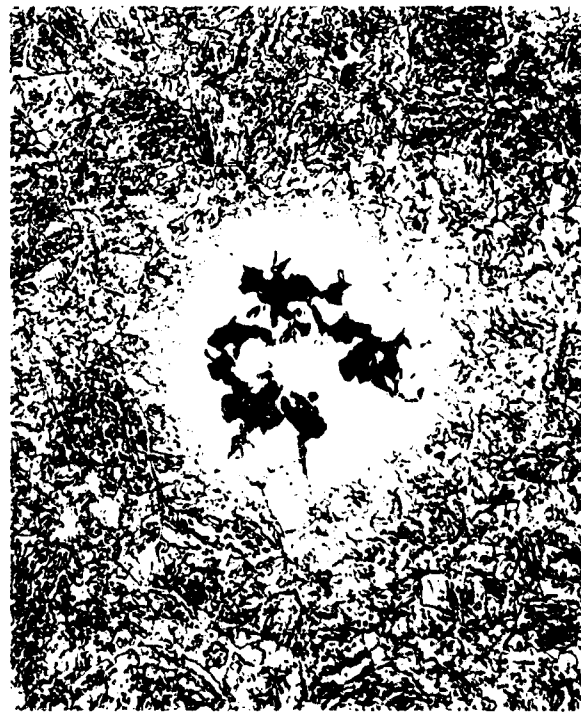
Differences in the microstructures of the three HIP'ed bars were also observed, as shown by the etched photomicrographs in Figures 8, 9, and 10. These microstructures were ferritic due to the slow cooling rate at the end of the HIP cycle. However, the two bars which had been HIP'ed previously at 1800°F (1260°K) and then re-HIP'ed at 2100°F (1420°K) exhibited coarser ferritic structures than the bar which was HIP'ed at 2100°F (1420°K) only. This difference was probably caused by the 1800°F (1260°K) HIP cycle, which imparted only a small amount of deformation to the powder



(a) Unetched, Magnification, 500X



(b) Etched, Magnification, 100X

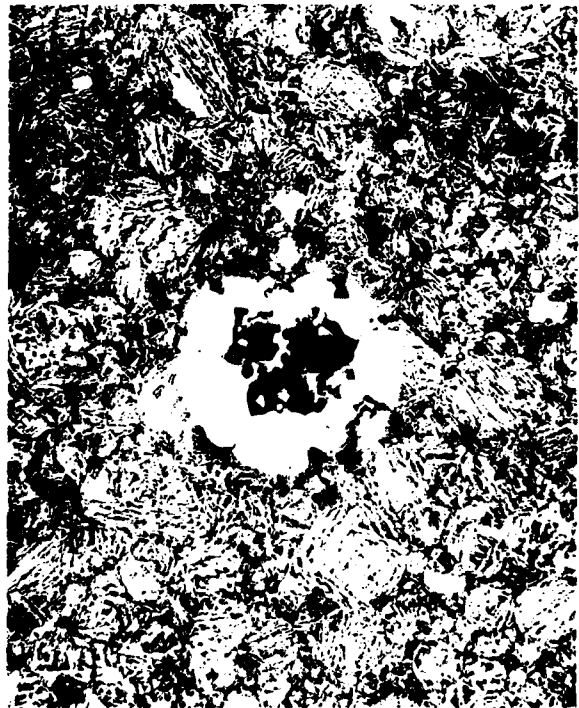


(c) Etched, Magnification, 500X

Figure 8. Light photomicrographs of as-HIP hydrogen gas atomized 4340 steel powder from Heat X989 (0.24% Ce) HIP'ed at 2100°F (1420°K).



(a) Unetched, Magnification, 500X



(b) Etched, Magnification, 100X

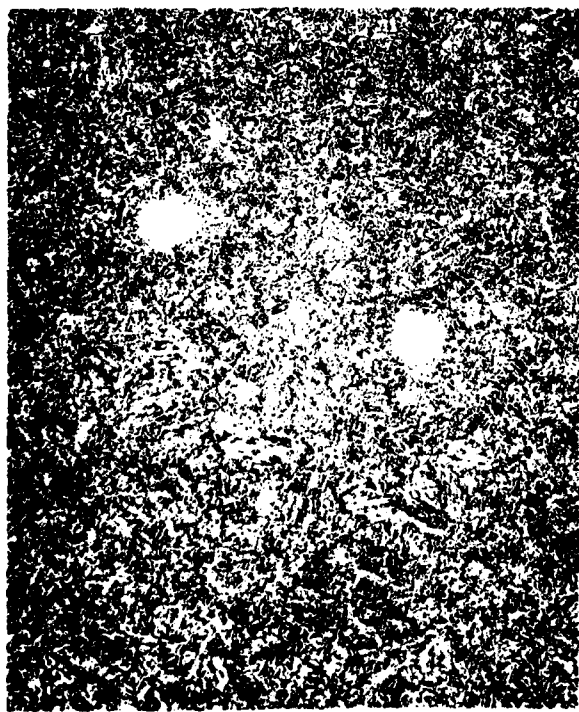


(c) Etched, Magnification, 500X

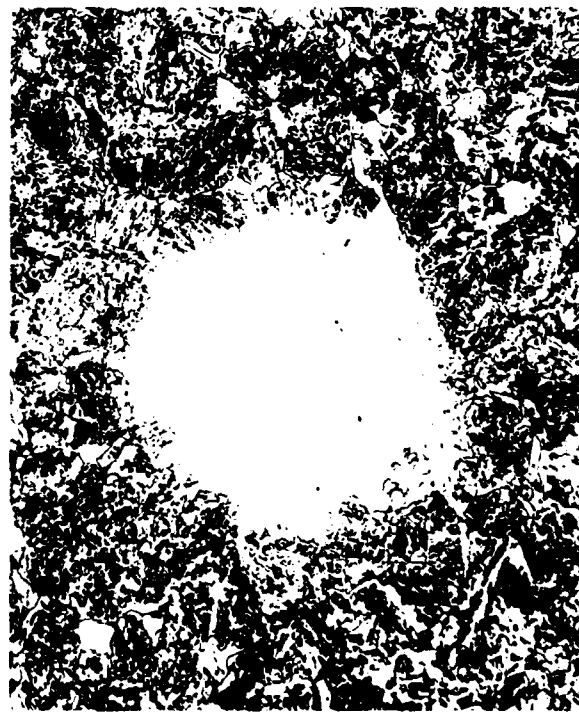
Figure 9. Light photomicrographs of as-HIP hydrogen gas atomized 4340 steel powder from Heat X916 (NoCe) HIP'ed at 1800°F (1260°K) and re-HIP'ed at 2100°F (1420°K).



(a) Unetched, Magnification, 500X



(b) Etched, Magnification, 100X



(c) Etched, Magnification, 500X

Figure 10. Light photomicrographs of as-HIP hydrogen gas atomized 4340 steel powders from Heat X971 (0.043% Ce) HIP'ed at 1800°F (1260°K) and re-HIP'ed at 2100°F (1420°K).

particles and thus resulted in a coarser austenite grain size after recrystallization. The coarser austenite grain size then resulted in the coarser ferritic structure upon transformation during cooling. Some additional coarsening of the ferritic structure probably occurred during the re-HIP cycle at 2100°F (1420°K). Conversely, the powder particles which were HIP'ed at 2100°F (1420°K) only were more heavily deformed, which resulted in a finer austenite grain size after recrystallization and in turn resulted in the finer ferritic structure upon transformation during cooling. In addition, the re-HIP'ed bar of heat X916 powder exhibited a coarser ferritic structure than the re-HIP'ed bar of heat X971 powder. This difference is believed to have been caused by differences in the microstructures of the powders from these two heats, since heat X916 was atomized with a mixture of 50% hydrogen and 50% argon. The addition of the argon to the atomizing gas for heat X971 probably altered the solidification rate of the powder particles and thus the microstructure of these particles.

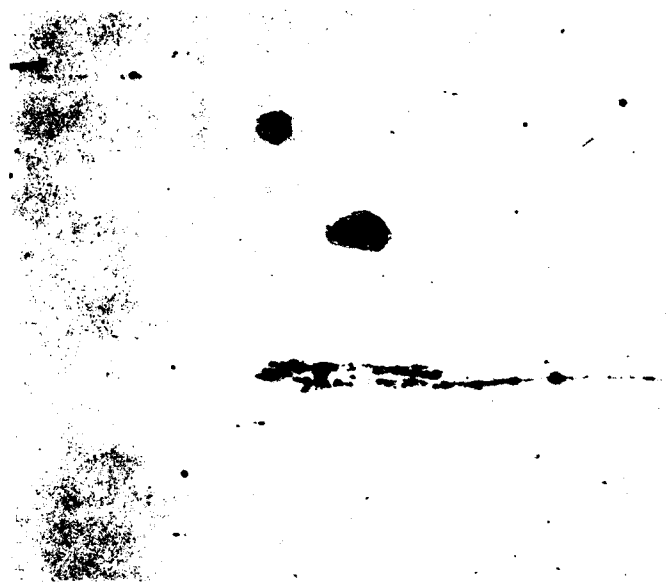
3.1.2.2.2 Hot Extrusion Consolidation

Photomicrographs of the bars which were extruded at 2150°F (1450°K) are shown in Figures 11 and 12 in the as-extruded condition. These two bars were extruded from powder from heat X917, which contained only 0.004% cerium, and heat X989, which contained 0.24% cerium. Both of these bars appeared to be completely compacted. However, both extrusions contained elongated oxide stringers oriented parallel to the longitudinal direction of the bar. An example of these stringers shown in the unetched photomicrographs in Figure 11 for the bar extruded from the powder having the high (0.24%) cerium content. This bar contained more of these stringers, suggesting that these were cerium oxide inclusions. Cross contamination particles were also observed in these two extrusions, but these were scattered sparsely in the microstructure. A difference in the microstructures of the two extruded bars was also observed, as shown by the etched photomicrographs in Figure 12. The microstructure of the heat X917 (0.004% Ce) bar was ferritic and bainitic (Figure 12a and b), whereas the microstructure of the heat X989 (0.24% Ce) bar was martensitic (Figure 12c and d), which is indicative of a faster cooling rate in this bar. This difference was attributed to the normal variation in cooling rate after extrusion, since the bars were discharged from the extrusion die into an insulated chamber and may not have been positioned similarly in the insulating material.

3.1.2.3 Powder Evaluation

3.1.2.3.1 HIP Powders

The mechanical properties of the bars which were HIP'ed or re-HIP'ed at 2100°F (1420°K) are presented in Table 3, along with the mechanical properties of wrought 4340 steel plates with and without cerium, heat treated the same way as the HIP'ed bars, evaluated previously⁽¹⁴⁾. As was the case for the bars HIP'ed at 2000°F (1370°K)⁽¹⁷⁾, the mechanical properties of the bars HIP'ed or re-HIP'ed at 2100°F (1420°K) were generally much lower than those of the wrought plates. The main exceptions to this were the yield and ultimate tensile strengths of the specimens from bars 9G254A, 9G254B, and 80B157, and one of the two specimens from bar 80B158. Also, the ultimate tensile strengths of the bars HIP'ed from powders from heats X916 and X989 showed considerable scatter. Most of the tensile specimens failed in such a brittle manner that it was not possible to obtain yield strength values for four of the specimens or to obtain any measurable elongation for six of

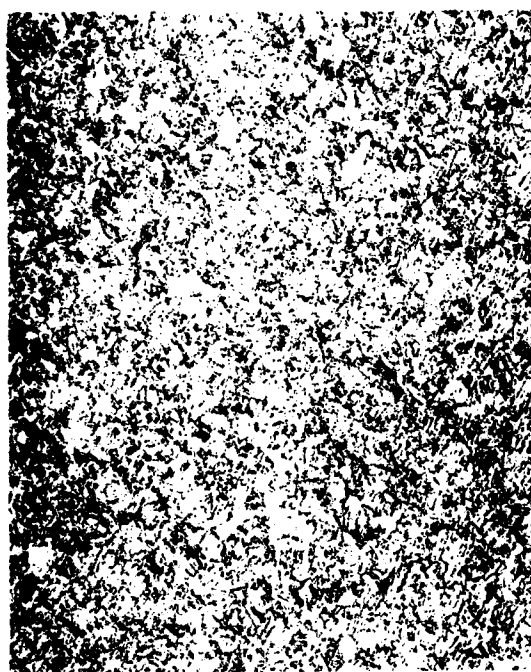


(a) Longitudinal section, Magnification, 100X



(b) Transverse section, Magnification, 100X

Figure 11. Light photomicrographs of unetched as-extruded hydrogen gas atomized 4340 steel powder from Heat X989 (0.24% Ce) extruded at 2150° F (1450° K) showing elongated oxide stringers.



(a) Heat X917 (0.004% Ce), Magnification, 100X



(b) Heat X917, Magnification, 500X



(c) Heat X989 (0.24% Ce), Magnification 100X



(d) Heat X989, Magnification, 500X

Figure 12. Light photomicrographs of etched longitudinal sections of as-extruded hydrogen gas atomized 4340 steel powders extruded at 2150° F (1450° K).

Table 3
Mechanical Properties of 4340 Steel HIP'ed Bars and Wrought Plates

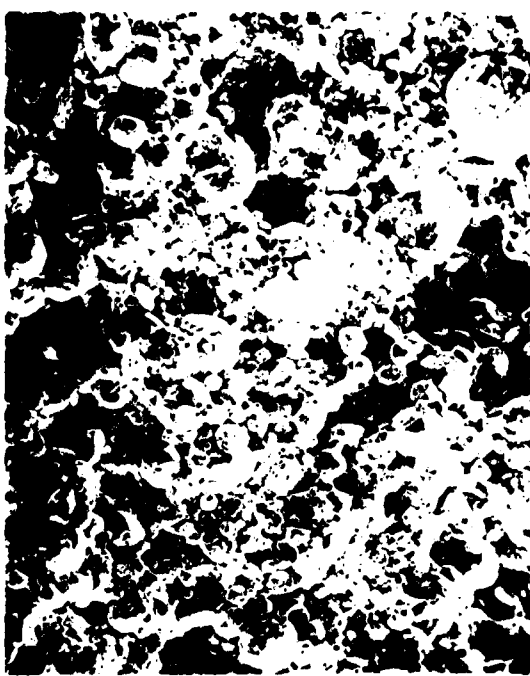
Heat/Bar No.	Cerium Content %	Yield Strength at 0.2% Offset Ksi	Ultimate Tensile Strength Ksi	Elongation %	Reduction of Area %	Charpy Impact Energy ft-lb		Charpy Impact Energy J	
						Bars HIP'ed at 1800°F (1160°K) and Re-HIP'ed at 2100°F (1420°K)	Bars HIP'ed at 2100°F (1420°K)	Bars HIP'ed at 2100°F (1420°K)	Bars HIP'ed at 2100°F (1420°K)
X916/9G253A	0	-	52.1	359	0	0	1.0	1.4	1.4
X916/9G253B	0	-	168	1160	0	0	1.0	1.4	1.4
X916/9G253B	0	-	187	1290	0	0	-	-	-
X971/9G254A	0.043	195	1340	266	1830	3.5	4.7	10.5	14.2
X971/9G254B	0.043	200	1380	261	1800	1.0	4.0	4.5	6.1
X989/80B157	0.24	196	1350	223	1540	0	0.4	1.5	2.0
X989/80B158	0.24	-	190	1310	0	0	1.5	2.0	2.0
X989/80B158	0.24	197	1360	210	1450	0	0	-	-
<u>Wrought Plates</u>									
X409	0	206	1420	254	1750	13.3	50.4	23.5	31.9
X421	0.17	200	1380	248	1710	10.3	34.7	10.5	14.2

the specimens. The fracture surfaces of these six tensile specimens were flat and granular in appearance, while the fracture surfaces of the two tensile specimens with measurable elongation (i.e., those from bars 9G254A and 9G254B) had a fibrous appearance and a small shear lip around the perimeter, similar to the appearance of the fracture surfaces of the tensile specimens from the wrought plates. The fracture surfaces of the Charpy impact specimens were similar to those of the tensile specimens taken from the same bars, i.e., they were flat and granular in appearance except for the fracture surfaces of the Charpy impact specimens from bars 9G254A and 9G254B, which had a fibrous appearance and small shear lips along the sides.

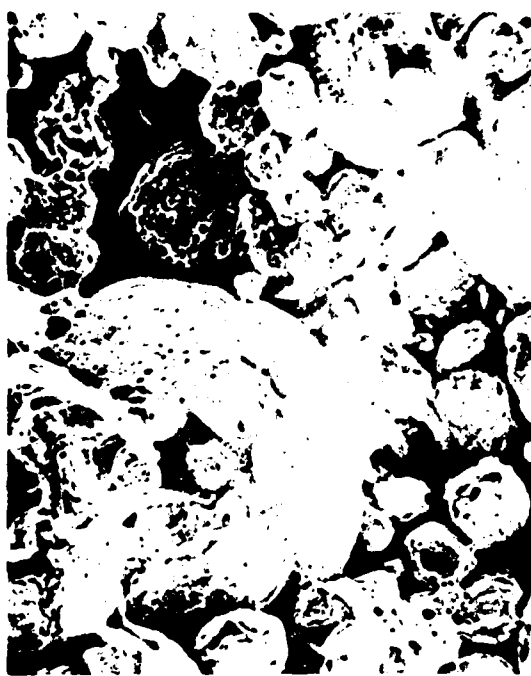
Fractographic examinations were performed on tensile specimens representing each of the three heats of powder HIP'ed or re-HIP'ed at 2100°F (1420°K). Scanning electron photomicrographs of the fracture surface of the tensile specimen from bar 9G253A are shown in Figure 13 a and b. This bar had been HIP'ed at 1800°F (1260°K) from heat X916 powder, which contained no cerium, and re-HIP'ed at 2100°F (1420°K). The tensile specimen from this bar failed at an ultimate tensile strength of 52.1 ksi (359 MPa) with no measurable elongation. The photographs in Figure 13a and b indicate that the fracture path was along prior particle boundaries, as the shapes of powder particles are clearly evident. Light photomicrographs of longitudinal section through the fracture surface of this specimen, shown in Figure 13c and d, confirm this observation. The particles appear to have been pulled apart during tensile testing.

SEM photographs of the fracture surface of the tensile specimens from bar 9G254A are shown in Figure 14a and b. This bar had been HIP'ed at 1800°F (1260°K) from heat X971 powder, which contained 0.043% cerium, and re-HIP'ed at 2100°F (1420°K). The tensile specimen from this bar failed at an ultimate tensile strength of 266 ksi (1830 MPa) after an elongation of 3.5% and exhibited a yield strength of 195 ksi (1340 MPa) at 0.2% offset. The photographs in Figure 14a and b indicate that the fracture mode was a mixture of intergranular separation and microvoid coalescence, as both grain or prior particle surfaces and ductile rupture dimples are evident. Light photomicrographs of a longitudinal section through the fracture surface of this specimen, shown in Figure 14c and d, support these observations. It was not clear whether the intergranular separation occurred along prior austenite grain boundaries or prior particle boundaries.

SEM photographs of the fracture surface of one of the two tensile specimens from bar 80B158 are shown in Figure 15a and b. This bar had been HIP'ed at 2100°F (1420°K) from heat X989 powder, which contained 0.24% cerium. This tensile specimen failed at an ultimate tensile strength of 190 ksi (1310 MPa) with no measurable elongation. The photographs in Figure 15a and b indicate that the fracture path was primarily intergranular, as most of the fracture surface consists of grain or prior particle surfaces. A significant amount of ductile rupture dimples are also present, indicating some degree of microvoid coalescence. The light photomicrographs of a longitudinal section through the fracture surface of this specimen, shown in Figure 15c and d, tend to support these observations. Again, it was not clear whether the intergranular separation occurred along prior austenite grain boundaries or prior particle boundaries. However, wrought 4340 steel in this heat treat condition does not normally fail along prior austenite grain boundaries in a room temperature tensile test⁽³¹⁾, so the intergranular separation most likely occurred along prior particle boundaries.



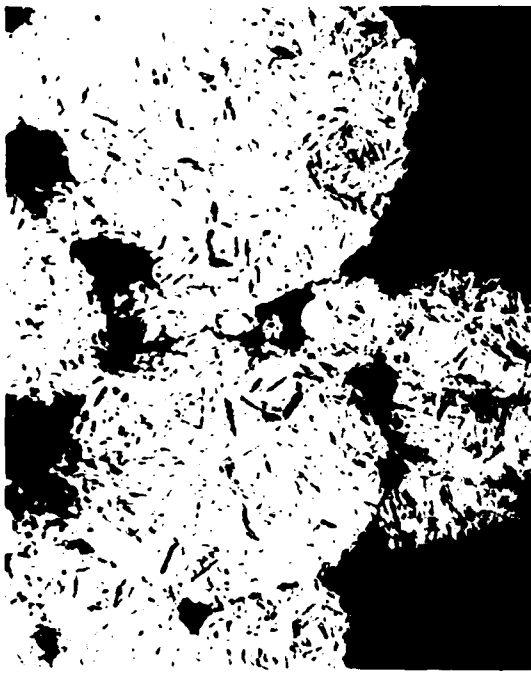
(a) SEM photo, Magnification, 100X



(b) SEM photo, Magnification, 500X

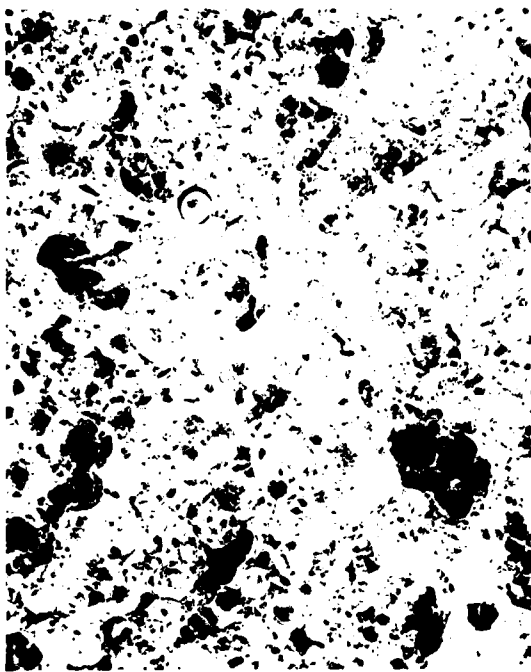


(c) Light photomicrograph, Magnification, 100X



(d) Light photomicrograph, Magnification, 500X

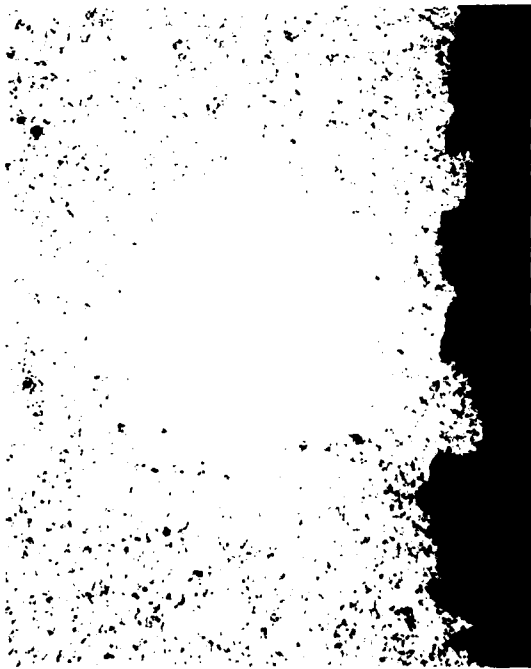
Figure 13. SEM photographs of fracture surface and light photomicrographs of longitudinal section through fracture surface of tensile specimen from bar 9G253A which was made of 4340 steel powder without cerium from Heat X916 HIP'ed at 1800° F (1260° K) and re-HIP'ed at 2100° F (1420° K).



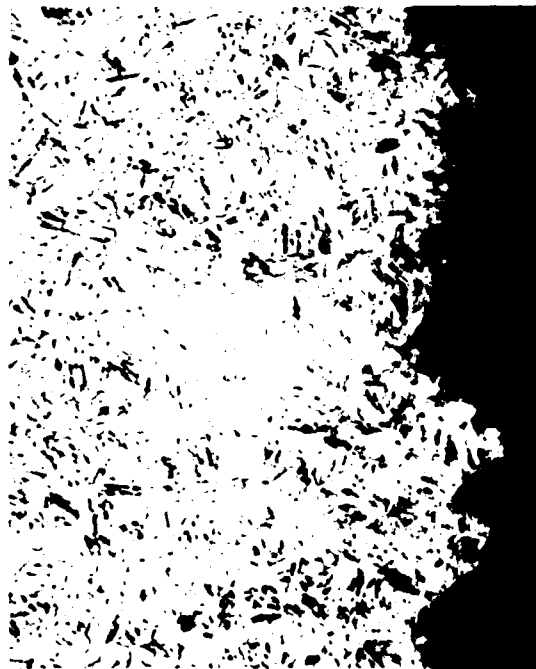
(a) SEM photo, Magnification, 100X



(b) SEM photo, Magnification, 500X

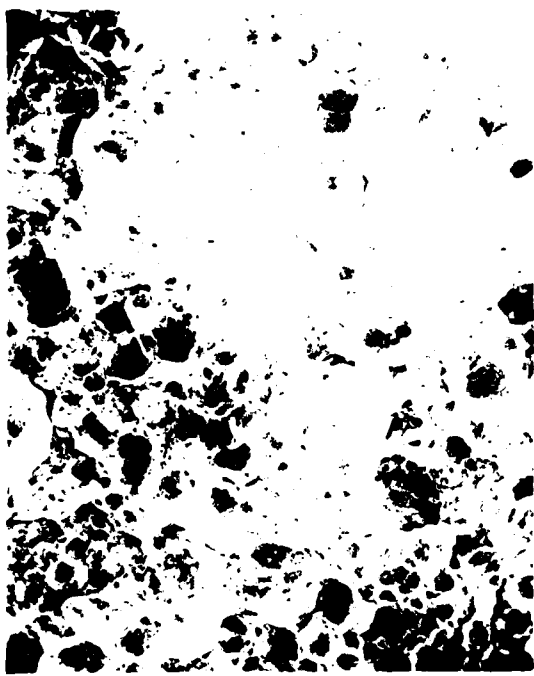


(c) Light photomicrograph, Magnification, 100X

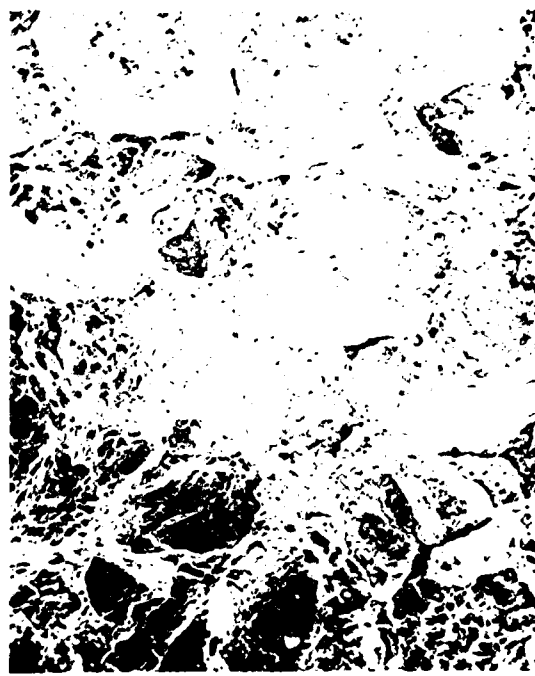


(d) Light photomicrograph, Magnification, 500X

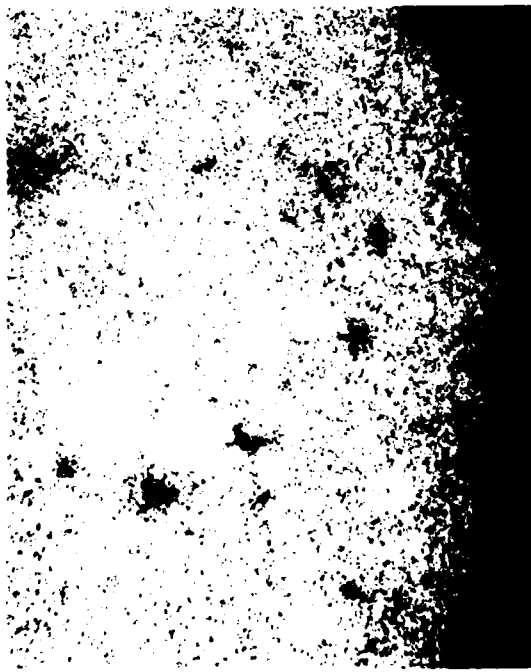
Figure 14. SEM photographs of fracture surface and light photomicrographs of longitudinal section through fracture surface of tensile specimen from bar 9G254A, which was made of 4340 steel powder with 0.043% Ce from Heat X971 HIP'ed at 1800°F (1260°K) and re-HIP'ed at 2100°F (1420°K).



(a) SEM photo, Magnification, 100X



(b) SEM photo, Magnification, 500X



(c) Light photomicrograph, Magnification, 100X



(d) Light photomicrograph, Magnification, 500X

Figure 15. SEM photographs of fracture surface and light photomicrographs of longitudinal section through fracture surfaces of tensile specimen from bar 80B158, which was made of 4340 steel powder with 0.24% C_e from Heat X989 HIP'ed at 2100° F (1420 K).

The cracking along the prior particle boundaries was indicative of a brittle condition in these boundaries. This condition was undoubtedly responsible for the poor mechanical properties of the HIP'ed bars, as well as the high degree of scatter in some of these properties. The fracture path did not appear to be associated with the cross contaminant particles observed in the microstructure after HIP (Figures 8, 9, and 10). The investigation of the cause of failure along the prior particle boundaries is continuing, and involves Auger electron spectroscopy of the fracture surfaces.

3.1.2.3.2 Extruded Powders

The mechanical properties of the bars which were extruded at 2150⁰F (1450⁰K) are presented in Table 4. Also shown in this table for comparison are the mechanical properties of the wrought 4340 steel plates with and without cerium, heat treated the same way as the extruded bars, evaluated previously⁽¹⁴⁾. In general, the mechanical properties of the extruded bars were substantially better than those of the HIP'ed bars, but still not as good as the properties of the wrought plates. Also, the mechanical properties of the extruded bars exhibited very little scatter. The yield strengths of the extruded bars were as high as those of the wrought plates, while the ultimate tensile strengths of the extruded bars were a little higher than those of the wrought plates. However, the elongations, reductions of area, and Charpy impact energies of the extruded bars were generally much lower than those of the wrought plates at approximately the same cerium content. An exception to this was the Charpy impact energy of bar 6 from heat X989 containing 0.24% cerium, which was higher than that of the wrought plate containing 0.17% cerium.

The fracture surfaces of the four tensile specimens from the extruded bars had a fibrous appearance and a shear lip around the perimeter, similar to the appearance of the fracture surfaces of the tensile specimens from the wrought plates. The fracture surfaces of the four Charpy impact specimens from the extruded bars had a fibrous appearance and small shear lips along the sides, also similar to the appearance of the fracture surfaces of the Charpy impact specimens from the wrought plates. Metallographic and fractographic analyses are currently being conducted to aid in the interpretation of these results.

3.1.3 Summary and Conclusions

The hydrogen gas atomization process was used to make four heats of 4340 steel powder containing zero, 0.004, 0.043 and 0.24% cerium. Light microscopy of the powders containing 0.043 and 0.24% cerium indicated that they were clean and relatively free of nonmetallic inclusions, similar to the powders containing zero and 0.004% cerium which had been characterized previously. No significant differences were observed in either the scanning electron microscope or the light microscope between the powders which contained 0.043 and 0.24% cerium. Electron microprobe analysis of the powder containing 0.24% cerium revealed that cerium was present in approximately 20 percent of the powder particles and was located more often at the surface of the particles than in the interior. The cerium in these particles was always concentrated in a very small area, suggesting the presence of a very small cerium-bearing phase, and was usually associated with a higher oxygen content than that in the remainder of the powder particle.

Table 4
Mechanical Properties of 4340 Steel Extruded Bars and Wrought Plates

<u>Heat/Bar No.</u>	<u>Cerium Content %</u>	<u>Yield Strength at 0.2% Offset Ksi</u>	<u>Ultimate Tensile Strength Ksi</u>	<u>Elongation %</u>	<u>Reduction of Area %</u>	<u>Charpy Impact Energy ft-lb</u>	<u>Charpy Impact Energy J</u>
<u>Bars Extruded at 2150°F (1450°K)</u>							
X917/5	0.004	206	1420	265	1830	10.0	37.0
X917/5	0.004	201	1390	264	1820	11.5	40.7
X989/6	0.24	205	1410	263	1810	7.5	17.6
X989/6	0.24	203	1400	262	1810	7.5	19.7
<u>Wrought Plates</u>							
X409	0	206	1420	254	1750	13.3	50.4
X421	0.17	200	1380	248	1710	10.3	34.7

Hydrogen gas atomized 4340 steel powder containing 0.24% cerium was consolidated by hot isostatic pressing (HIP) at a pressure of 15,000 psi (103 MPa) and a temperature of 2100°F (1420°K) for 2 hours, as previous HIP processing at 1800 and 2000°F (1260 and 1370°K) had proved to be unsatisfactory. In addition, bars of powders containing zero and 0.043% cerium which had been HIP'ed previously at 1800°F (1260°K), were re-HIP'ed at 2100°F (1420°K). Some evidence of incomplete compaction was observed in all of these HIP'ed or re-HIP'ed bars, but this condition did not appear to be extensive. Cross contamination particles containing a number of extraneous elements were also observed in these bars. Samples of these bars were heat treated by normalizing, austenitizing, quenching, and tempering at 450°F (505°K), the same heat treatment used for wrought plates of rare earth modified 4340 steel evaluated previously. The mechanical properties of the bars HIP'ed or re-HIP'ed at 2100°F (1420°K) and heat treated were generally much lower than those of the wrought plates, and the fracture modes were generally brittle and intergranular. These results were attributed to a brittle condition in the prior particle boundaries. The fracture path did not appear to be associated with the cross contaminant particles. The investigation of the cause of failure along the prior particle boundaries is continuing.

Because of the poor mechanical properties obtained with the HIP process, hot extrusion was included in the program for powder consolidation. Hydrogen gas atomized 4340 steel powders containing 0.004 and 0.24% cerium were extruded at a temperature of 2150°F (1450°K) and an extrusion ratio of 16:1 to produce round bars. The extruded bars appeared to be completely compacted, but contained elongated oxide stringers oriented parallel to the longitudinal direction of the bar. The bar having the high (0.24%) cerium content contained more of these stringers, suggesting that these were cerium oxide inclusions. Cross contamination particles were also observed in the extruded bars. The yield and ultimate tensile strengths of these bars after heat treatment were as high as or a little higher than those of the wrought plates, but the ductility and impact resistance were generally much lower than those of the wrought plates at approximately the same cerium content, except the impact energy of the 0.24% cerium extrusion which was higher than the 0.17% cerium plate. These results are currently being analyzed in terms of metallography and fractography.

3.2 Mechanical Alloying

3.2.1 Experimental Procedures

3.2.1.1 Powder Preparation

The mechanical alloying process involves subjecting a blend of powders to highly energetic compressive impact forces, such as those occurring in a high energy stirred ball mill, shaker mill, or vibratory ball mill⁽²⁰⁻²²⁾. The starting charge usually consists of a blend of elemental, master alloy, and compound powders of very different characteristics and initial particle sizes. Interdispersion of the ingredients occurs by repeated cold welding and fracturing of the powder particles. The mechanical alloying process is unique in that it is an entirely solid state process, allowing dispersion of insoluble phases such as refractory oxides and addition of reactive alloying elements such as aluminum and titanium.

As reported previously⁽¹⁷⁾, preliminary mechanical alloying experiments were conducted by attriting hydrogen gas atomized 4340 steel powder containing no rare earths with rare earth compound granules in a Szegvari Pilot Laboratory Model No. 1-S

Attritor. An attritor is a high energy stirred ball mill in which the charge of balls and powder is held in a stationary, vertical, water cooled tank and agitated by impellers radiating from a rotating central shaft. Six preliminary attriting runs were conducted and in five of these runs, cerium or lanthanum was added as 75% cerium - 25% nickel alloy granules or LaNi_5 alloy granules, respectively. The objective was to obtain a uniform distribution of the rare earth additions in the microstructure of the steel. The attriting process was not effective in the first five runs, as indicated by only slight deformation of the powder particles. This result was attributed to the hardness of the steel powder particles as a result of rapid cooling during atomization. Annealing of the steel powder at 1200°F (920°K) for 2 hours in a vacuum prior to attriting in the sixth run resulted in effective attriting, as indicated by heavy deformation of the powder particles.

During the second year of the program, four final attriting runs were conducted with sufficient powder for subsequent consolidation and mechanical property evaluation. The master alloy powder used in these final attriting runs was commercially rapidly solidified (CRS) 4340 steel powder from heat Q483, containing no rare earths, which is described later in the section on rapid solidification atomization. CRS powder was utilized for this purpose because of the availability of a large quantity of this powder in conjunction with the study of rapidly solidified powders. No significant differences in the mechanical alloying results were anticipated as a result of using CRS powder instead of hydrogen gas atomized powder.

The CRS powder was annealed at 1200°F (920°K) for 2 hours in a vacuum prior to attriting. A Szegvari Intermediate Model No. 10-S Attritor was employed for these attriting runs. The conditions used in these four runs are given in Table 5. The mass of the steel powder charge was 10 lbs (4.5 kg.) in each of these runs. Cerium or lanthanum was added to the starting charge for three of these runs in the form of 75% cerium - 25% nickel alloy granules or LaNi_5 alloy granules, respectively. No rare earths were added to the starting charge for run 9, as this was used for a control sample. The amounts of cerium and lanthanum added to the starting charge for runs 7, 8, and 10 represented an increase over the amount (0.3%) of cerium or lanthanum added in the preliminary attriting runs because rare earth losses of 40 to 70 percent occurred in the preliminary runs, resulting in a rare earth content of only about 0.1% in the attrited powders. However, despite the addition of 0.5% cerium in run 7, the resulting cerium content of the attrited powder was only 0.10%. This run was therefore repeated as run 10, with the cerium addition doubled to 1.0%, but the resulting cerium content of the attrited powder only increased to 0.12%. These rare earth losses were attributed to the ineffective action of the impellers at the bottom of the attritor tank, as discussed later. The grinding balls used in all four final runs were 1/4-inch (0.0064-m.) diameter carbon steel balls. The mass of the grinding balls used in each of these runs was 200 lbs. (91 kg.), resulting in a ball/powder ratio of 20:1 for all of these runs. All four final attriting runs were conducted in an atmosphere of argon gas to minimize oxidation of the metal powder particles.

3.2.1.2 Powder Consolidation

Attrited powders from runs 8, 9, and 10 were consolidated by hot extrusion at a temperature of 2150°F (1450°K) and an extrusion ratio of 16:1, using the procedure described earlier for the hydrogen gas atomized powders. Hot extrusion was employed for consolidating the attrited powders rather than HIP because hot extrusion had resulted in

Table 5
Final Attriting of 4340 Steel Powder

Run Number	Rare Earth Addition	Grinding Ball Diameter Inches (m)	Attriting Time Hours		Rare Earth Content of Powder	Oxygen Content of Powder ppm
			1/4 (0.0064)	32		
7	0.5% Ce	1/4 (0.0064)			0.10% Ce	950
8	0.5% La	1/4 (0.0064)			0.22% La	1300
9	-	1/4 (0.0064)			-	1800
10	1.0% Ce	1/4 (0.0064)			0.12% Ce	1800

much better mechanical properties for the hydrogen gas atomized powders than HIP. The extrusion operation produced round bar stock measuring 3/4-inch (0.019-m.) in diameter by approximately 36-inches (0.91-m.) long. The net diameter of the extruded 4340 steel bar was 5/8-inch (0.016-m.) after the can material was removed by machining on a lathe. One extrusion was made from each of the three runs of attrited powders.

3.2.1.3 Powder Evaluation

The extruded bars were evaluated by metallographic analysis and mechanical property tests on heat treated specimens. The metallographic analyses were performed on 1/4-inch (0.0064-m.) thick slices cut from the bars. The mechanical properties of these bars were evaluated by performing duplicate tensile and Charpy impact tests at room temperature on specimens machined from the bars. Two tensile specimens and two Charpy impact specimens were taken from each of the three extruded bars. The dimensions of these test specimens are shown in Figure 4. These specimens were rough machined from the extruded bars, heat treated, and then finish ground to their final dimensions. The heat treatment was the same as that used for the compacted bars of hydrogen gas atomized powders, which was described earlier.

3.2.2 Results and Discussion

3.2.2.1 Powder Characterization

During the second year of the program, an electron microprobe analysis was performed on the powder from the sixth preliminary attriting run, which had resulted in effective attriting and a cerium content of 0.10% in the attrited powder. This analysis showed that cerium was present in approximately 20 percent of the powder particles and was located as often in the interior of the particles as at the surface. The cerium in these particles was more uniformly distributed than that in the hydrogen gas atomized powder containing 0.24% cerium, indicating a high degree of mechanical alloying, and was usually associated with a higher oxygen content than that in the remainder of the particle. As reported previously⁽¹⁷⁾, the oxygen content of this powder increased during attriting from 142 ppm in the starting charge to 880 ppm in the attrited powder, and this increase was attributed to pick-up of residual oxygen in the argon atmosphere used in the attriting operation.

The results of the four final attriting runs are presented in Table 5. The rare earth contents of the attrited powders from the three runs in which rare earths were added were only 12 to 44 percent of the rare earth contents of the starting charges, indicating that much of the rare earth additions were lost during attriting. These losses are believed to have occurred at the bottom of the attritor tank where the impellers are less effective. These losses were probably much larger than would normally be expected because the charge sizes in these attriting runs were much smaller than the capacity of the attritor tank, which was 15 gallons (57 liters). The attriting operation increased the oxygen content of the steel powder from 330 ppm in the starting charge to levels of 950 to 1800 ppm in the attrited powders. This increase in oxygen content was probably due to residual oxygen which was present in the argon atmosphere and was picked up by the steel powder particles and the rare earth additive particles.

Light photomicrographs of the as-received CRS powder and typical attrited powder particles are shown in Figure 16. The attrited particles shown in Figure 16b were from the control sample, run 9, which contained no rare earths. No differences in the microstructures of the attrited powders from runs 8, 9, and 10 could be discerned by light microscopy. The microstructures of the particles from these runs were heavily deformed, indicating that the attriting process was effective.

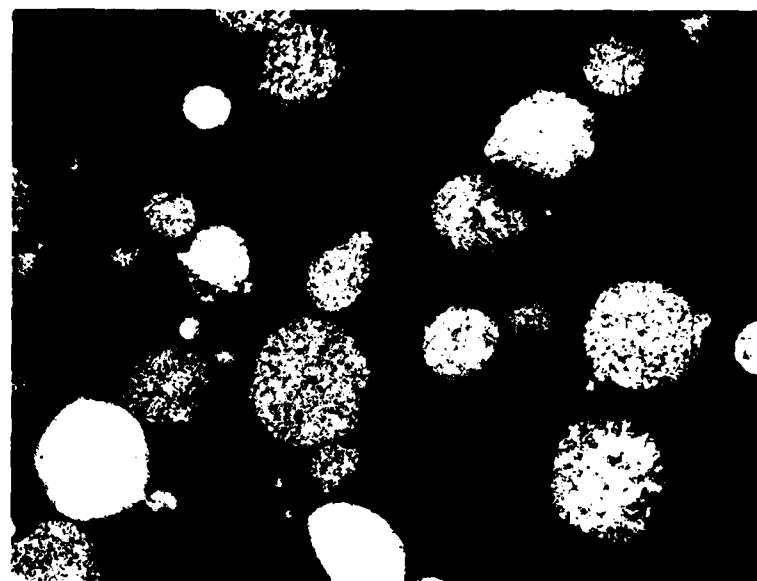
3.2.2.2 Powder Consolidation

Photomicrographs of the as-extruded bars are shown in Figures 17 and 18. These three bars were extruded from attrited powders containing (1) 0.22% lanthanum, (2) no rare earths, and (3) 0.12% cerium. All of these bars appeared to be completely compacted. However, all three extrusions contained elongated oxide stringers oriented parallel to the longitudinal direction of the bar, as shown in the unetched photomicrographs in Figure 17. These stringers were much smaller than those observed in the extruded bars of hydrogen gas atomized powders discussed earlier. The bar extruded from the powder attrited with no rare earths contained about as many of these stringers as the other two bars, which suggested that these were not rare earth oxide inclusions. These stringers are currently being analyzed. No significant differences were observed among the microstructures of the three extruded bars, and the microstructure shown in Figure 18 was typical of all three bars.

3.2.2.3 Powder Evaluation

The mechanical properties of the extruded bars are presented in Table 6. For comparison, the mechanical properties of the wrought 4340 steel plates with and without cerium, which had been heat treated the same way as the extruded bars and were evaluated previously^[14], are also shown in this table. The yield and ultimate tensile strengths of these extruded bars were higher than those of the wrought plates and also higher than those of the bars extruded from hydrogen gas atomized powders (Table 4). However, the elongations, reductions of area, and Charpy impact energies of these extruded bars were generally much lower than those of the wrought plates as well as those of the extruded bars of hydrogen gas atomized powders (Table 4) at approximately the same rare earth content. The mechanical properties of the extruded bars of attrited powders exhibited little scatter. Also, the rare earth additions had no significant effect on the yield and ultimate tensile strengths and Charpy impact energy, slightly decreased the elongation, and moderately decreased the reduction of area.

The fracture surfaces of the six tensile specimens from these extruded bars had a fibrous appearance and a shear lip around the perimeter, similar to the appearance of the fracture surfaces of the tensile specimens from the wrought plates. The fracture surfaces of the six Charpy impact specimens from these extruded bars had a fibrous appearance and small shear lips along the sides, also similar to the appearance of the fracture surfaces of the Charpy impact specimens from the wrought plates. The reason for the lower ductility and impact resistance of these extruded bars, as compared with the wrought plates and the hydrogen gas atomized powder extrusions, is currently being investigated.



(a) As-received CRS 4340 powder



(b) As-attrited powder from run 9

Figure 16. Light photomicrographs of etched attrited powder particles from attriting run 9, compared to as-received CRS 4340 powder. Magnification, 100X.

(a) No rare earth addition

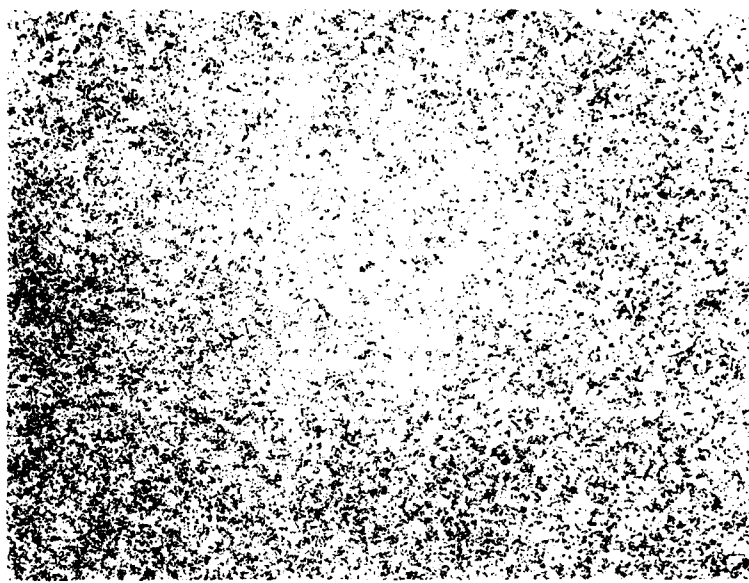


(b) 0.22% lanthanum

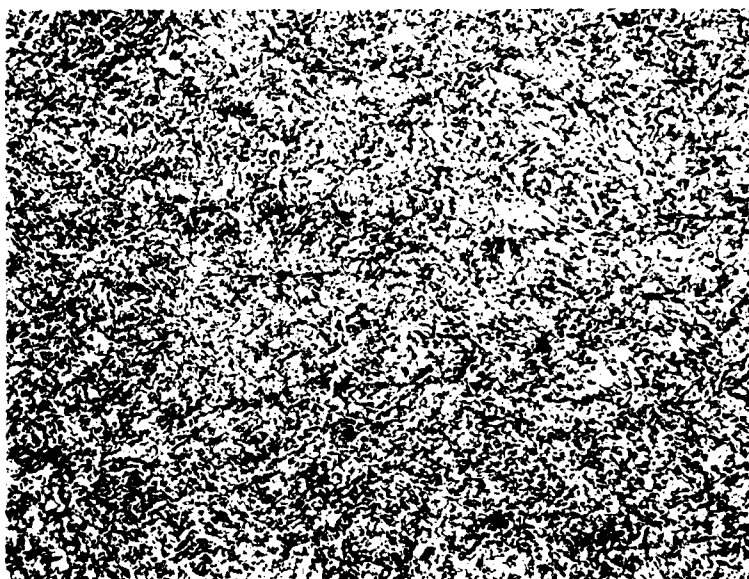


(c) 0.12% cerium

Figure 17. Light photomicrographs of unetched longitudinal section of as-extruded 4340 powders attrited for 32 hours and extruded at 2150°F (1450°K) showing elongated oxide stringers. Magnification, 500X.



(a) Magnification, 100X



(b) Magnification, 500X

Figure 18. Light photomicrographs of etched longitudinal sections of as-extruded 4340 powder of attrition run 10 (0.12% Ce) extruded at 2150° F (1450° K).

Table 6
**Mechanical Properties of 4340 Steel Attrited Powder/Extruded Bars
 and Wrought Plates**

<u>Bar Number</u>	<u>Rare Earth Content</u>	<u>Yield Strength at 0.2% Offset</u>		<u>Ultimate Tensile Strength</u>		<u>Elongation %</u>	<u>Reduction of Area %</u>	<u>Charpy Impact Energy ft-lb</u>	<u>Charpy Impact Energy J</u>
		<u>Ksi</u>	<u>MPa</u>	<u>Ksi</u>	<u>MPa</u>				
<u>Bars Extruded at 2150°F (1450°K) From Attrited Powder</u>									
9	0.22% La	225	1550	277	1910	6.0	14.7	7.5	10.2
9	0.22% La	222	1530	274	1890	7.5	17.5	7.5	10.2
10	0	224	1540	273	1880	7.5	21.8	8.0	10.8
10	0	228	1570	271	1870	8.6	24.6	7.0	9.5
11	0.12% Ce	231	1590	277	1910	1.0	15.1	5.5	7.5
11	0.12% Ce	220	1520	276	1900	5.0	9.4	6.0	8.1
<u>Wrought Plates</u>									
X409	0	206	1420	254	1750	13.3	50.4	23.5	31.9
X421	0.17% Ce	200	1380	248	1710	10.3	34.7	10.5	14.2

3.2.3 Summary and Conclusions

Mechanical alloying of commercially rapidly solidified (CRS) 4340 steel powder containing no rare earths with rare earth compound granules was accomplished using a Szegvari Attritor. Electron microprobe analysis of attrited powder which contained 0.10% cerium and was the product of a preliminary attriting run showed that cerium was present in approximately 20 percent of the powder particles and was located as often in the interior of the particles as at the surface. The cerium in these particles was more uniformly distributed than that in the hydrogen gas atomized 4340 steel powder which contained 0.24% cerium, indicating a high degree of mechanical alloying, and was usually associated with a higher oxygen content than that in the remainder of the particle. Four final attriting runs were conducted in which annealed CRS 4340 steel powder was attrited with (1) 75% Ce - 25% Ni (two runs), (2) LaNi₅, and (3) no rare earths for control purposes. Rare earth losses of 56 to 88 percent occurred in the attrited powders, and these losses were attributed to the small charge size in comparison with the capacity of the attritor tank. The oxygen content of the steel powder increased during attriting from 330 ppm in the starting charge to levels of 950 to 1800 ppm in the attrited powders, and this increase was attributed to pick-up of residual oxygen in the argon atmosphere used in the attriting operation.

Attrited 4340 steel powders containing 0.12% cerium, 0.22% lanthanum, and no rare earths were consolidated by hot extrusion at a temperature of 2150°F (1450°K) and an extrusion ratio of 16:1 to produce round bars. The extruded bars appeared to be completely compacted, but contained elongated oxide stringers oriented parallel to the longitudinal direction of the bar. The bar extruded from the powder attrited without rare earths contained about as many of these stringers as the other two bars, which suggested that these were not rare earth oxide inclusions. The yield and ultimate tensile strengths of these bars after heat treatment were higher than those of similarly heat treated, rare earth modified, wrought 4340 steel plates evaluated previously, but the ductility and impact resistance were generally much lower than those of the wrought plates at approximately the same rare earth content. The reason for these lower properties is currently being investigated.

3.3 Rapid Solidification Atomization

3.3.1 Experimental Procedures

Two different processes for making rapidly solidified powders were examined: rapid solidified rate (RSR) atomization and commercial rapid solidification (CRS) atomization, and these are described below

3.3.1.1 RSR Atomization

The RSR process involves centrifugal atomization of a liquid metal stream combined with forced convective cooling of the atomized droplets/particles using helium gas (24-26). Cooling rates on the order of 10^6 °F/second (5.6×10^9 °K/second) are achieved with this process, and these rates virtually freeze the molten metal into a supersaturated solid solution. The advantages anticipated in RSR powders, in addition to greater chemical homogeneity, are (1) an increase in the solubility limits of solute elements, (2) the formation of non-equilibrium structures, (3) large undercooling prior to solidification, and (4) the formation of amorphous structures in certain alloy systems.

As reported previously⁽¹⁷⁾, a control heat of 4340 steel powder containing no rare earth elements was made by the RSR atomization process at Pratt & Whitney Aircraft, Government Products Division, while another RSR heat of 4340 steel powder containing 0.2% cerium was in preparation. The melt stock for the control heat of RSR powder was obtained from an ingot of vacuum arc remelted 4340 steel. This ingot was converted to RSR powder in the Pratt & Whitney Aircraft AGT 500,000 atomization unit. This operation yielded a total of 12.1 lbs (5.5 kg.) of powder, including 6.7 lbs, (3.0 kg.) of -140 mesh powder or 55 percent of the total powder yield.

The melt stock for the cerium-bearing heat of RSR powder was obtained by making a 45-lb. (20-kg.) ingot of 4340 steel with no rare earth addition, similar to those used for hydrogen gas atomization⁽¹⁷⁾. The chemical composition of this ingot is given in Table 7. This ingot was machined to the size and shape required by Pratt & Whitney Aircraft⁽¹⁷⁾ to fit into the melting crucible in their RSR atomization facilities, as described previously. In addition, four holes were drilled in one end of the machined ingot to accommodate the cerium-nickel alloy additive, in order to ensure thorough mixing of this additive with the molten steel, since no provision was available for adding alloying elements to the melt just before atomization on any of the RSR atomization units at Pratt & Whitney Aircraft. The cerium-nickel additive, in the form of 75% cerium - 25% nickel alloy granules, the same material used for making the cerium additions in the hydrogen gas atomized powders, was poured into these four holes, and the holes were closed with threaded carbon steel plugs which were tack welded in place to prevent movement. Sufficient 75% Ce-25% Ni was added to obtain a cerium content of 0.2 weight percent in the resulting powder, assuming a cerium recovery of 20 percent, the same degree of recovery that was observed for the hydrogen gas atomized powders. During the second year of the program, this ingot was converted to RSR powder in the larger AGT 400,000 atomization unit at Pratt & Whitney Aircraft, using the same procedure as that used for the control heat, which was described previously⁽¹⁷⁾. This operation yielded 15.1 lbs (6.86-kg.) of -80 mesh powder.

3.3.1.2 CRS Atomization

The CRS process is a recent modification of the gas atomization process which increases the effective solidification rate of the powder and produces powders with characteristics similar to RSR powders. This process was developed by Universal-Cyclops Specialty Steel Division, Cyclops Corporation, as a more economical alternative to the expensive RSR process for making rapidly solidified powders. The CRS process is essentially a gas atomization operation with the processing parameters altered to significantly increase the proportion of fine powder (100 microns in diameter). The yield of -140 mesh (105 microns) powder is 80 percent of the input charge⁽³²⁾.

Two heats of rapidly solidified 4340 steel powder were made by the CRS atomization process, using nitrogen as the atomizing gas, at Universal-Cyclops under subcontract to TRW during the second year of the program. One of these heats was to contain 0.2 percent cerium and the other no rare earth addition for control purposes. These operations yielded 60 lbs. (27-kg.) of -80 mesh powder for the control heat (Q483) and 40 lbs (18-kg.) of -150 mesh powder for the cerium-bearing heat (Q484).

Table 7
Chemical Composition of RSR 4340 Steel Heat No. RSR 485
Weight Percent

<u>Element</u>	<u>AISI 4340 Specification</u>	<u>Vacuum-Induction Melted Ingot</u>	<u>RSR Atomized Powder</u>
(Heat No.)	-	Y627	RSR 485
C	0.38-0.43	0.40	0.40
Mn	0.60-0.80	0.76	0.36
P	0.040 max.	< 0.008	0.005
S	0.040 max.	0.005	0.005
Si	0.20-0.35	0.32	0.30
Ni	1.65-2.00	1.85	1.90
Cr	0.70-0.90	0.84	0.88
Mo	0.20-0.30	0.26	0.27
Al	-	0.043	0.015
O	-	-	0.013
N	-	-	0.0004
Ce	-	-	0.0019

3.3.2 Results and Discussion

3.3.2.1 RSR Atomization

The chemical composition of the cerium-bearing heat of RSR 4340 steel powder is given in Table 7. This heat was intended to contain 0.2 percent cerium, but it contained only 0.0019 percent cerium. This very low cerium recovery was attributed to vaporization of the cerium during melting of the ingot and subsequent superheating of the melt up to 2925°F (1880°K), since the melting range of the 75% Ce - 25% Ni alloy additive is only about 920 to 1150°F (770 to 900°K)⁽³³⁾. The high superheat was necessary because of the thermal characteristics of the RSR atomizing system. Because no provision was available for adding alloying elements to the melt just before atomization on any of the RSR atomization units at Pratt & Whitney Aircraft, this problem could not be resolved within the scope of this program, and no further work was performed on the RSR process.

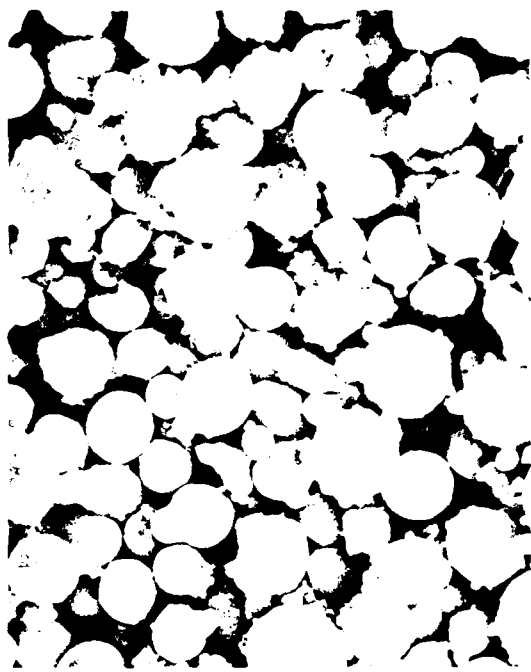
Scanning electron photomicrographs of samples of the loose powders from the two heats of CRS 4340 steel are shown in Figure 19. The powder particles were generally spherical in shape, which is typical of powders made by the CRS atomization process, but result of collisions with other particles or the chamber walls. However, much less flake was present in the CRS powders than in the hydrogen gas atomized powders. Most of the CRS particles appeared to have smaller satellite particles attached to them, similar to the hydrogen gas atomized 4340 steel powder particles (Figures 5 and 6). The solidification patterns on the surfaces of the CRS powder particles were equiaxed, also similar to the hydrogen gas atomized powder particles. These patterns are indicative of a similarity in heat flow during atomization of the two types of powders.

Light photomicrographs of both unetched and etched powder particles from the two heats of CRS 4340 steel are shown in Figure 20. The unetched photomicrographs indicate that these powders were clean and relatively free of nonmetallic inclusions, similar to the hydrogen gas atomized 4340 steel powder (Figure 7). The CRS powder particles also contained very few internal voids. The etched photomicrographs show that the microstructures of the CRS powders consisted of untempered martensite, which is typical of quenched 4340 steel and was observed previously in both the hydrogen gas atomized and RSR 4340 steel powders⁽¹⁷⁾. No differences in the microstructures of these three types of powder could be discerned in the light microscope.

The chemical compositions of the two heats of CRS 4340 steel powder are given in Table 8. The cerium-bearing CRS heat was intended to contain 0.2 percent cerium, but it contained only 0.01 percent cerium. The very low cerium recovery was attributed to oxidation of the cerium due to an inadequate vacuum level in the melting chamber. Because this difficulty could not be resolved within the scope of this program, no further work was performed on the CRS process.

3.3.3 Summary and Conclusions

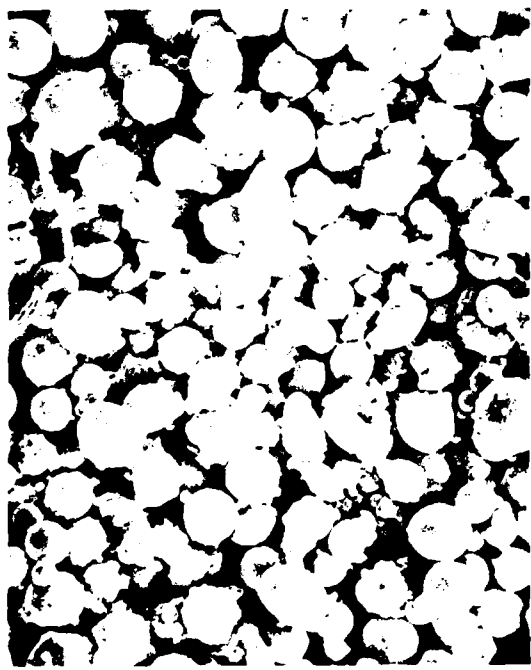
Two different processes for making cerium-modified, rapidly solidified 4340 steel powder were examined: rapid solidification rate (RSR) atomization and commercial rapid solidification (CRS) atomization. Two heats of rapidly solidified 4340 steel powder were



(a) Heat Q483, Magnification, 100X



(b) Heat Q483, Magnification, 500X

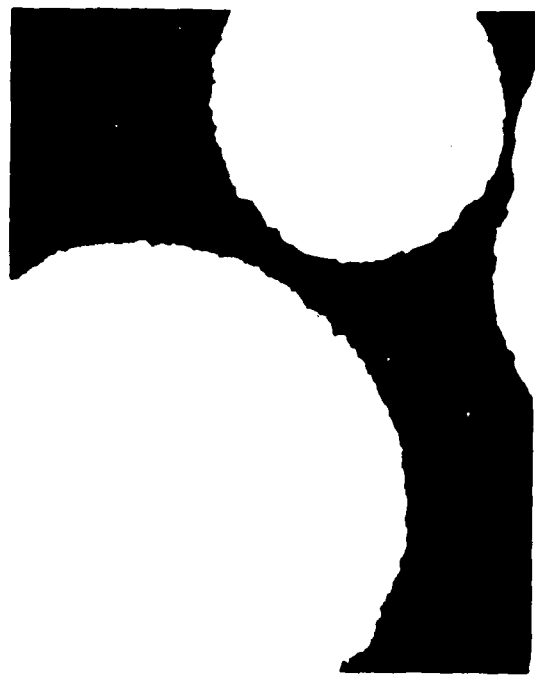


(c) Heat Q484, Magnification, 100X

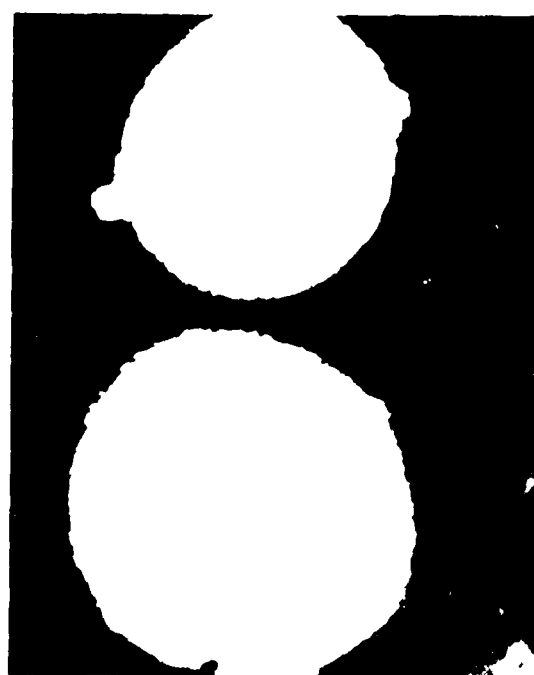


(d) Heat Q484, Magnification, 500X

Figure 19. SEM photographs of CRS atomized 4340 steel powders.



(a) Heat Q483, Unetched



(b) Heat Q484, Unetched



(c) Heat Q483, Etched



(d) Heat Q484, Etched

Figure 20. Light photomicrographs of CRS atomized 4340 steel powders. Magnification, 500X.

Table 8

Chemical Compositions of CRS 4340 Steel Powders
Weight Percent

<u>Element</u>	<u>AISI 4340 Specification</u>	<u>Heat No. Q483</u>	<u>Heat No. Q484</u>
C	0.38-0.43	0.45	0.41
Mn	0.60-0.80	0.62	0.34
P	0.040 max.	0.015	0.015
S	0.040 max.	0.018	0.018
Si	0.20-0.35	0.20	0.07
Ni	1.65-2.00	1.84	1.94
Cr	0.70-0.90	0.99	1.00
Mo	0.20-0.30	0.26	0.30
O	-	0.033	0.036
N	-	0.14	0.13
Ce	-	-	0.01

made by each process, one heat of which was to contain 0.2 percent cerium and the other no rare earth addition for control purposes. However, both cerium-bearing heats contained very little cerium (0.0019% in the RSR heat and 0.01% in the CRS heat). The very low cerium recovery in the RSR heat was attributed to vaporization of the cerium during melting of the charge and subsequent superheating of the melt, since it was necessary to add the cerium prior to heating the charge. The very low cerium recovery in the CRS heat was attributed to oxidation of the cerium due to an inadequate vacuum level in the melting chamber. Because these difficulties could not be resolved within the scope of this program, no further work was performed on rapidly solidified powders.

4.0 FUTURE WORK

This program is concerned with the development of powder metallurgy methods for producing rare earth modified high strength 4340 steel with improved resistance to hydrogen embrittlement. The powder metallurgy approach offers a means of obtaining a more uniform distribution of the rare earth elements in the microstructure of the steel, compared with the wrought 4340 steel plate investigated previously, and thus improved mechanical properties and hydrogen embrittlement resistance. The work conducted during the first year of the program involved studies of material processing techniques for producing rare earth modified 4340 steel from metal powders. In this work, three different methods of making the metal powders were explored; hydrogen gas atomization, mechanical alloying, and rapid solidification atomization. During the second year of the program, which was covered in this report, these material processing studies were continued. During the third year of the program, the material processing studies involving hydrogen gas atomization and mechanical alloying will be completed and the hydrogen embrittlement resistance of rare earth modified 4340 steel produced from powders made by these two methods will be evaluated. The work planned for the third year is described in the following sections.

4.1 Evaluation of Powder Processing

This investigation of the cause of failure along the prior particle boundaries in the tensile and Charpy impact tests of the hydrogen gas atomized powder materials HIP'ed at 2000 and 2100°F (1370 and 1420°K) will be completed. In addition, the investigation of the cause of the low ductility and impact resistance of the extruded bars made from both hydrogen gas atomized powders and mechanically alloyed powders will be completed. These investigations will include metallographic analyses, electron microprobe analyses, and scanning electron microscopy and Auger electron spectroscopy of fracture surfaces, as required. Depending on the results of these investigations, the powder processing operations will be modified to improve the mechanical properties of the powder metallurgy steels. For example, if it is found that the brittle condition in the prior particle boundaries of the HIP'ed material is due to an oxide film on the powder particles, the powder could be sintered at a high temperature in a reducing atmosphere to remove this film. If this brittle condition is due to chemical segregation, a heat treatment could be devised to homogenize the material.

4.2 Selection of Optimum Powder Processing Conditions

The material processing studies will be concluded with the selection of the optimum powder processing conditions. This selection will be made on the basis of the metallographic and mechanical property evaluations of the consolidated powder metallurgy steels, as well as the results of the specimen failure analyses described above.

4.3 Hydrogen Embrittlement Evaluation

4.3.1 Delayed Failure Testing

The hydrogen embrittlement cracking resistance of the powder metallurgy 4340 steels will be evaluated in this portion of the program. These evaluations will be conducted on steels processed according to three different conditions. Baseline testing will be

conducted on steel powders produced without rare earth additions. The other two conditions will be selected on the basis of the studies involving the optimization of processing parameters. It is anticipated that representative material will be selected from rare earth modified hydrogen gas atomized and mechanically alloyed powders at a single rare earth content. The optimum powder processing conditions established during the processing studies will be used to prepare the test materials. These conditions will be selected on the basis of (1) the resultant homogeneity of the rare earth elements distributed throughout the microstructure and (2) the mechanical property levels established during characterization of Charpy impact and tensile properties of the most promising materials. Prior to hydrogen embrittlement evaluations, however, the material will first be characterized by duplicate tensile and Charpy impact tests conducted on fully heat treated materials. These specimens will be heat treated to a yield strength level of approximately 200 ksi (1400 MPa) by austenitizing, quenching and tempering at 450°F (505°K) for comparison with results obtained during the processing parameter study. It is anticipated that a total of six Charpy impact and eight tensile tests will be conducted during this portion of the program.

The hydrogen embrittlement resistance of the rare earth modified steel will be determined by conducting sustained-load delayed failure tests on hydrogen charged and cadmium plated specimens. This type of delayed failure test was selected because the entire test system is "closed" with respect to metal-environment interactions, thus minimizing the possible entrance of external hydrogen which could influence the results. The specimen configuration utilized for these tests will be the notched round specimen. A single hydrogen charging condition selected on the basis of previous studies at TRW on high strength steel landing gears⁽³⁴⁾ will be used on these specimens to produce a highly embrittling condition within the steels. Complete delayed failure curves will be obtained for each of the three material conditions selected for the program. It is anticipated that a minimum of 10 specimens will be required for each condition thus resulting in a total of 30 notched round specimens for this portion of the program.

The results of the delayed failure testing on the powder metallurgy 4340 steel should provide an indication of the effect of hydrogen getter additions on its hydrogen embrittlement resistance compared to the rare earth modified 4340 wrought plate material. If it can be demonstrated that the rare earths increase the crack initiation time or decrease the crack propagation rate in hydrogenated powder metallurgy 4340, then it may also be possible to demonstrate similar benefits in other alloys or specimens exposed to hydrogen containing environments.

4.3.2 Hydrogen Content Analysis

The purpose of this portion of the program is to develop an improved understanding of the ability of the rare earth additions to inhibit hydrogen embrittlement in high strength steels produced by powder metallurgy techniques. If it is assumed, for example, that hydrogen trapping or gettering by the rare earth additions is the operative mechanism, once failure has occurred in the hydrogenated and plated specimens, the uncombined hydrogen can diffuse through the matrix and exit through the fresh fracture surface. If the hydrogen has been trapped by the rare earth getters, however, it is unable to diffuse through the metal matrix and remains instead in some combined form within the specimen. The experimental approach to study this possibility will involve obtaining hydrogen contents of specimens after failure. Since all specimens have been charged and

plated with the same conditions, the differences in the hydrogen contents may reflect the fact that the rare earth additives have trapped hydrogen, thus reducing its ability to embrittle the material.

The experimental procedure for the hydrogen content measurements will include utilization of the Boeing-developed "Ultra-sensitive Hydrogen Analysis System." This system works on the principle of selective permeation of hydrogen through a semi-permeable metallic membrane. Details regarding operating procedure, range, and accuracy of the instrumentation have been described previously⁽³⁵⁾. Briefly, specimens are stored in liquid nitrogen immediately after failure to minimize hydrogen loss from the fractured surfaces. Just prior to localized hydrogen measurements on fractured surfaces, the specimens are removed from the liquid nitrogen and thawed at room temperature under blowing dry argon gas. Thereafter, specimens from the desired areas of fractured surfaces are obtained by careful slow cutting of sections under an argon atmosphere, such an operation for high strength steels usually taking about 30 to 45 minutes per sample. For this program, the hydrogen analyses on the fractured surfaces will be carried out in the following two areas for each specimen: (1) slow crack growth regions, and (2) base metal (a region opposite to the fractured surface, but not including the fractured surface). It is anticipated that a minimum of six specimens will undergo analysis in this portion of the program. Duplicate specimens will be selected from baseline material as well as rare earth modified hydrogen gas atomized and mechanically alloyed powder metallurgy specimens.

4.3.3 Fractographic and Auger Analyses

The objective of this part of the program is to ascertain whether the microstructural aspects of the mechanism of hydrogen induced crack growth in powder metallurgy steels are altered by the addition of rare earth elements. In particular, the work will assist in understanding how the *more homogeneous distribution* of the rare earth additions can effect the hydrogen embrittlement resistance of these materials. In this program, metallographic analyses will be performed using light metallography, the scanning electron microscope and the electron microprobe on the notched round specimens tested under conditions to induce internal hydrogen embrittlement. Fractographic studies will be conducted using the scanning electron microscope. Auger electron spectroscopy of the fracture surfaces will be utilized to study the effects of local composition variations on hydrogen-induced crack propagation. This technique has proved to be valuable in understanding the role of grain boundary impurities in hydrogen-induced cracking in high strength steels⁽³⁶⁾. Specimen selection will be made on the basis of the delayed failure results, with representative analyses being made on baseline material and rare earth modified hydrogen gas atomized and mechanically alloyed powder metallurgy specimens. It is anticipated that a minimum of 15 specimens will be analyzed in this portion of the program.

5.0 REFERENCES

1. Third International Conference on Effect of Hydrogen on Behavior of Materials, Jackson Lake Lodge, Wyoming, August 26-29, 1980, proceedings to be published by AIME.
2. I. M. Bernstein and A. W. Thompson, "Effect of Metallurgical Variables on Environmental Fracture of Steels," Intl. Metals Reviews, December 1976, pp. 269-287.
3. H. H. Johnson, J. G. Morlet, and A. R. Troiano, "Hydrogen, Crack Initiation, and Delayed Failure in Steel," Trans. AIME, Vol. 212, August 1978, pp. 528-536.
4. W. Beck and E. J. Jankowsky, "Effects of Plating High Tensile Strength Steels," Proc. American Electroplaters Society, Vol. 44, 1957, pp. 47-52.
5. W. Beck and E. J. Jankowsky, "The Effectiveness of Metallic Undercoats in Minimizing Plating Embrittlement of Ultra High Strength Steel," Proc. American Electroplaters Society, Vol. 47, 1960, pp. 152-159.
6. L. H. McEowan and A. R. Elsea, "Behavior of High Strength Steels under Cathodic Protection," Corrosion, Vol. 21, 1965, pp. 28-37.
7. F. N. Speller, Corrosion, Causes and Prevention, 3rd Edition, McGraw-Hill, New York, 1951, pp. 320-376.
8. R. P. Wei and G. W. Simmons, "Environment Enhanced Fatigue Crack Growth in High-Strength Steels," Technical Report No 1, Contract N00014-67-A-03700008, NR 036-097, March 1973
9. H. W. Liu, Ya-lung Hu, and P. J. Ficalora, "The Control of Catalytic Poisoning and Stress Corrosion Cracking," Eng. Fracture Mech., Vol. 5, No. 2, June 1973, pp. 281-292.
10. E. I. Nikolaev, Yu. V. Kryakovskii, E. I. Tyurin, and V. I. Yanoiskii, "Chemical Heterogeneity and Nonmetallic Inclusions in Steel Ingots Containing Rare Earth Metals," Izv., VUZ-Chern. Met., 1965, (7), pp. 37-42, English Translation, H. Brutcher, No. 6626.
11. H. Homma, "A Study of Delayed Cracking in HY-80 Weldments," Ph.D. Thesis, Rensselaer Polytechnic Institute, 1973.
12. W. F. Savage, "The Effect of Rare Earth Additions on Hydrogen-Induced Cracking in HY-80 Weldments," Presented at the International Symposium on Sulfide Inclusions in Steel, 7-8 November 1974, Port Chester, New York
13. M. D. Hayes and D. Hauser, "Hydrogen in HY-130 Weld Metal," Battelle Columbus Laboratories report prepared for ONR Contract No. N00014-74-C-0407, May 14, 1979

14. C. S. Kortovich, "Inhibition of Hydrogen Embrittlement in High Strength Steel," TRW Technical Report No. ER-7814-2, prepared for ONR Contract No. N00014-74-C-0365, February 1977.
15. A. A. Sheinker, "Effect of Rare Earth Additions on Stress Corrosion Cracking of 4340 Steel," TRW Technical Report No. ER-7814-3, prepared for ONR Contract No. N00014-74-C-0365, January 1978.
16. A. A. Sheinker, "Effect of Rare Earth Additions on Hydrogen Embrittlement Cracking in 4340 Steel," TRW Technical Report No. ER-7814-4, prepared for ONR Contract No. N00014-74-C-0365, October 1978.
17. A. A. Sheinker, "Rare Earth Modified High Strength Steels via P/M Processing," TRW Technical Report No. ER-8097, prepared for ONR Contract No. N00014-78-C-0672, December 1979.
18. J. M. Wentzell, "Metal Powder Production by Vacuum Atomization," J. Vac. Sci Technol., Vol. 11, No. 6, Nov./Dec. 1974, pp. 1035-1037.
19. P. Rao, R. Grandzol, N. Schultz, and J. A. Tallmadge, "Quench Atomization of Iron Base Alloys into Metal Powders," Presented at International Conference on Vacuum Metallurgy, Anaheim, California, 15-19 June 1970.
20. J. S. Benjamin, "Dispersion Strengthened Superalloys by Mechanical Alloying," Met. Trans., Vol. 1 No. 10, October 1970, pp. 2943-2951.
21. J. S. Benjamin and T. E. Volin, "The Mechanism of Mechanical Alloying," Met. Trans., Vol. 5, No. 8, August 1974, pp. 1929-1934.
22. J. S. Benjamin, "Mechanical Alloying," Scientific American, May 1976, pp. 40-48.
23. J. J. Reilly and G. D. Sandrock, "Hydrogen Storage in Metal Hydrides," Scientific American, February 1980, pp. 118-129.
24. A. R. Cox, "Application of Rapidly Solidified Superalloys," Pratt & Whitney Aircraft Report FR-7627, First Quarterly Report for DARPA Contract F33615-76-C-5136, May 1976.
25. A. R. Cox, J. B. Moore and E. C. Van Reuth, "On the Rapid Solidification of Superalloys," Superalloys: Metallurgy and Manufacture, B. H. Kear et al, eds., Claitor's Publishing Division, Baton Rouge, La., 1976, pp. 45-53.
26. P. R. Holiday, A. R. Cox and R. J. Patterson II, "Rapid Solidification on Alloy Structures," Rapid Solidification Processing: Principles and Technologies, R. Mehrabian et al, eds., Claitor's Publishing Division, Baton Rouge, La., 1978, pp. 246-257.
27. H. D. Hanes, "Hot Isostatic Processing," High-Pressure Science and Technology, Vol 2, K. D. Timmerhaus and M. S. Barber, eds., Plenum Publishing Corp., New York, 1979, pp. 633-650.

28. J. S. Hirschhorn, Introduction to Powder Metallurgy, American Powder Metallurgy Institute, 1969.
29. G. H. Gessinger and M. J. Bomford, "Powder Metallurgy of Superalloys." Intl. Met. Rev., Vol. 19, June 1974, pp. 51-75.
30. E. N. Bamberger, J. S. Mosier, and R. W. Harrison, "Materials for Advanced Turbine Engines," General Electric Co. Report No. R78AEG265, Eighth Quarterly Engineering Report for NASA Contract NAS-3-20074, March 31, 1978.
31. F. R. Larson and F. L. Carr, "Tensile Fracture Surface Configurations of a Heat Treated Steel as Affected by Temperature," ASM Trans. Quarterly, Vol. 55, No. 3, September 1962, p. 599.
32. Personal communication, W. B. Kent, Universal-Cyclops Specialty Steel Division, Cyclops Corp., Bridgeville, Pa., Nov. 1980.
33. K. A. Gschneidner, Jr., and M. E. Verkade, "Selected Cerium Phase Diagrams," Report No. IS-RIC-7, Rare Earth Information Center, Energy and Mineral Resources Research Institute, Iowa State University, Ames, Iowa, September 1974.
34. G. M. Waid, "Stress Corrosion and Hydrogen Embrittlement Studies of Ultra-High Strength Steels (HP310, 4340, 300M)," Republic Steel Research Center Report P. R. 12049-76-4, September, 1976.
35. K. B. Das, "An Ultrasensitive Hydrogen Detector," Hydrogen Embrittlement Testing, ASTM STP 543, American Society for Testing and Materials, Philadelphia, 1974, pp. 106-112.
36. S. K. Banerji, C. J. McMahon, Jr., and H. C. Feng, "Intergranular Fracture in 4340-Type Steels: Effects of Impurities and Hydrogen," Met. Trans. A, Vol. 9A, No. 2, February 1978, pp. 237-247.

BASIC DISTRIBUTION LIST

Technical and Summary Reports

<u>Organization</u>	<u>Copies</u>	<u>Organization</u>	<u>Copies</u>
Defense Documentation Center Cameron Station Alexandria, Virginia 22314	12	Naval Air Propulsion Test Center Trenton, New Jersey 08628 Attention: Library	1
Office of Naval Research Department of the Navy 800 N. Quincy Street Arlington, Virginia 22217		Naval Construction Battalion Civil Engineering Laboratory Port Hueneme, California 93043 Attention: Materials Division	1
Attention: Code 471	1	Naval Electronics Laboratory San Diego, California 92152 Attention: Electron Materials Sciences Division	1
Code 102	1		
Code 470	1		
Commanding Officer Office of Naval Research Branch Office Building 114, Section D 666 Summer Street Boston, MA 02210	1	Naval Missile Center Materials Consultant Code 3312-1 Point Mugu, California 92041	1
Commanding Officer Office of Naval Research 536 South Clark Street Branch Office Chicago, Illinois 60605	1	Commanding Officer Naval Surface Weapons Center White Oak Laboratory Silver Spring, Maryland 20910 Attention: Library	1
Office of Naval Research San Francisco Area Office One Hallidie Plaza, Suite 601 San Francisco, California 94102	1	David W. Taylor Naval Ship Research and Development Center Materials Department Annapolis, Maryland 21402	1
Naval Research Laboratory Washington, D.C. 20375		Naval Undersea Center San Diego, California 92132 Attention: Library	1
Attention: Codes 6000	1	Naval Underwater System Center Newport, Rhode Island 02840 Attention: Library	1
6100	1		
6300	1		
6400	1		
2627	1	Naval Weapons Center China Lake, California 93555	
Naval Air Development Center Code 302 Warminster, Pennsylvania 18964 Attention: Mr. F. S. Williams	1	Attention: Library	1
		Naval Postgraduate School Monterey, California 93940 Attention: Mechanical Engineering Department	1

BASIC DISTRIBUTION LIST (continued)

<u>Organization</u>	<u>Copies</u>	<u>Organization</u>	<u>Copies</u>
Naval Air Systems Command Washington, D.C. 20360 Attention: Codes 52031 52032	1 1	NASA Headquarters Washington, D.C. 20546 Attention Code RRM	1
Naval Sea System Command Washington, D.C. 20362 Attention: Code 035	1	NASA Lewis Research Center 21000 Brookpark Road Cleveland, Ohio 44135 Attention: Library	1
Naval Facilities Engineering Command Alexandria, Virginia 22331 Attention: Code 03	1	National Bureau of Standards Washington, D.C. 20234 Attention: Metallurgy Division Inorganic Materials Div.	1
Scientific Advisor Commandant of the Marine Corps Washington, D.C. 20380 Attention: Code AX	1	Director Applied Physics Laboratory University of Washington 1013 Northeast Fortieth Street Seattle, Washington 98105	1
Naval Ship Engineering Center Department of the Navy Washington, D.C. 20360 Attention: Code 6101	1	Defense Metals and Ceramics Information Center Battelle Memorial Institute 505 King Avenue Columbus, Ohio 43201	1
Army Research Office P.O. Box 12211 Triangle Park, North Carolina 27709 Attention: Metallurgy & Ceramics Program	1	Metals and Ceramics Division Oak Ridge National Laboratory P.O. Box X Oak Ridge, Tennessee 37380	1
Army Materials and Mechanics Research Center Watertown, Massachusetts 02172 Attention: Research Programs Office	1	Los Alamos Scientific Laboratory P.O. Box 1663 Los Alamos, New Mexico 87544 Attention: Report Librarian	1
Air Force Office of Scientific Research Building 410 Bolling Air Force Base Washington, D.C. 20332 Attention: Chemical Science Directorate Electronics & Solid State Sciences Directorate	1 1 1	Argonne National Laboratory Metallurgy Division P.O. Box 229 Lemont, Illinois 60439	1
		Brookhaven National Laboratory Technical Information Division Upton, Long Island New York 11973 Attention: Research Library	1

BASIC DISTRIBUTION LIST (continued)

<u>Organization</u>	<u>Copies</u>	<u>Organization</u>	<u>Copies</u>
Air Force Materials Laboratory Wright-Patterson AFB Dayton, Ohio 45433	1	Office of Naval Research Branch Office 1030 East Green Street Pasadena, California 91106	1
Library Building 50, Room 134 Lawrence Radiation Laboratory Berkeley, California	1		

SUPPLEMENTARY DISTRIBUTION LIST

Technical and Summary Reports

Dr. T. R. Beck
Electrochemical Technology Corporation
10035 31st Avenue, NE
Seattle, Washington 98125

Professor I. M. Bernstein
Carnegie-Mellon University
Schenley Park
Pittsburgh, Pennsylvania 15213

Professor H. K. Birnbaum
University of Illinois
Department of Metallurgy
Urbana, Illinois 61801

Dr. Otto Buck
Rockwell International
1049 Camino Dos Rios
P.O. Box 1085
Thousand Oaks, California 91360

Dr. David L. Davidson
Southwest Research Institute
8500 Culebra Road
P.O. Drawer 28510
San Antonio, Texas 78284

Dr. D. J. Duquette
Department of Metallurgical Engineering
Rensselaer Polytechnic Institute
Troy, New York 12181

Professor R. T. Foley
The American University
Department of Chemistry
Washington, D.C. 20016

Mr. G. A. Gehring
Ocean City Research Corporation
Tennessee Avenue & Beach Thorofare
Ocean City, New Jersey 08226

Dr. J. A. S. Green
Martin Marietta Corporation
1450 South Rolling Road
Baltimore, Maryland 21227

Professor R. H. Heidersbach
University of Rhode Island
Department of Ocean Engineering
Kingston, Rhode Island 02881

Professor H. Herman
State University of New York
Material Sciences Division
Stony Brook, New York 11970

Professor J. P. Hirth
Ohio State University
Metallurgical Engineering
1314 Kinnear Road
Columbus, Ohio 43212

Dr. E. W. Johnson
Westinghouse Electric Corporation
Research and Development Center
1310 Beulah Road
Pittsburgh, Pennsylvania 15235

Professor R. M. Latanision
Massachusetts Institute of Technology
77 Massachusetts Avenue
Room E19-702
Cambridge, Massachusetts 02139

Dr. F. Mansfeld
Rockwell International Science Center
1049 Camino Dos Rios
P.O. Box 1085
Thousand Oaks, California 91360

Dr. Jeff Perkins
Naval Postgraduate School
Monterey, California 93940

SUPPLEMENTARY DISTRIBUTION LIST (continued)

Professor H. W. Pickering
Pennsylvania State University
Department of Material Sciences
University Park, Pennsylvania 16802

Dr. E. A. Starke, Jr.
Georgia Institute of Technology
School of Chemical Engineering
Atlanta, Georgia 30332

Dr. Barry C. Syrett
Stanford Research Institute
333 Ravenswood Avenue
Menlo Park, California 94025

Dr. R. P. Wei
Lehigh University
Institute for Fracture and
Solid Mechanics
Bethlehem, Pennsylvania 18015

Professor H. G. F. Wilsdorf
University of Virginia
Department of Materials Science
Charlottesville, Virginia 22903

Dr. Clive Clayton
State University of New York
Material Sciences Division
Stony Brook, New York 11970

END
DATE
FILMED

2 8/1

DTIC